




Article

Activating SIRT-1 Signalling with the Mitochondrial-CoQ10 Activator Solanesol Improves Neurobehavioral and Neurochemical Defects in Ouabain-Induced Experimental Model of Bipolar Disorder

Bidisha Rajkhowa¹, Sidharth Mehan^{1,*}, Pranshul Sethi¹, Aradhana Prajapati¹, Manisha Suri¹, Sumit Kumar¹, Sonalika Bhalla¹, Acharan S. Narula², Abdulrahman Alshammari³, Metab Alharbi³, Nora Alkahtani³, Saeed Alghamdi³ and Reni Kalfin^{4,5}

- ¹ Division of Neuroscience, Department of Pharmacology, ISF College of Pharmacy, Moga 142001, India; bidishadhunu@gmail.com (B.R.); pranshulsethiptl@gmail.com (P.S.); aradhanapjt@gmail.com (A.P.); manishasuri9015@gmail.com (M.S.); sumitsrivastav223@gmail.com (S.K.); sonalikabhalla97@gmail.com (S.B.)
- ² Narula Research, LLC, 107 Boulder Bluff, Chapel Hill, NC 27516, USA; acharannarula@icloud.com
- ³ Department of Pharmacology and Toxicology, College of Pharmacy, King Saud University, P.O. Box 2455, Riyadh 11451, Saudi Arabia; abdalshammari@ksu.edu.sa (A.A.); mesalharbi@ksu.edu.sa (M.A.); 441203710@student.ksu.edu.sa (N.A.); smalghamdi@sfh.med.sa (S.A.)
- ⁴ Institute of Neurobiology, Bulgarian Academy of Sciences, Acad. G. Bonchev St., Block 23, 1113 Sofia, Bulgaria; reni_kalfin@abv.bg
- ⁵ Department of Healthcare, South-West University “Neofit Rilski”, Ivan Mihailov St. 66, 2700 Blagoevgrad, Bulgaria
- * Correspondence: sidh.mehan@gmail.com; Tel.: +91-8059889909



Citation: Rajkhowa, B.; Mehan, S.; Sethi, P.; Prajapati, A.; Suri, M.; Kumar, S.; Bhalla, S.; Narula, A.S.; Alshammari, A.; Alharbi, M.; et al. Activating SIRT-1 Signalling with the Mitochondrial-CoQ10 Activator Solanesol Improves Neurobehavioral and Neurochemical Defects in Ouabain-Induced Experimental Model of Bipolar Disorder. *Pharmaceuticals* **2022**, *15*, 959. <https://doi.org/10.3390/ph15080959>

Academic Editors: Shaohua Hu and Gary J. Stephens

Received: 21 June 2022

Accepted: 27 July 2022

Published: 2 August 2022

Publisher's Note: MDPI stays neutral with regard to jurisdictional claims in published maps and institutional affiliations.



Copyright: © 2022 by the authors. Licensee MDPI, Basel, Switzerland. This article is an open access article distributed under the terms and conditions of the Creative Commons Attribution (CC BY) license (<https://creativecommons.org/licenses/by/4.0/>).

Abstract: Bipolar disorder (BD) is a chronic mental illness characterized by mood fluctuations that range from depressive lows to manic highs. Several studies have linked the downregulation of SIRT-1 (silent mating type information regulation-2 homologs) signaling to the onset of BD and other neurological dysfunctions. This research aimed to look into the neuroprotective potential of Solanesol (SNL) in rats given ICV-Ouabain injections, focusing on its effect on SIRT-1 signaling activation in the brain. Ouabain, found in hypothalamic and medullary neurons, is an endogenous inhibitor of brain Na⁺/K⁺ ATPase. The inhibition of brain Na⁺/K⁺ ATPase by Ouabain may also result in changes in neurotransmission within the central nervous system. SNL is a Solanaceae family active phytoconstituent produced from the plant *Nicotiana tabacum*. SNL is used as a precursor for the production of CoQ10 (Coenzyme Q10), a powerful antioxidant and neuroprotective compound. In the current study, lithium (Li), an important mood stabilizer drug, was used as a control. This study looked at the neuroprotective potential of SNL at dosages of 40 and 80 mg/kg in ICV-OUA injections that caused BD-like neurobehavioral and neurochemical defects in Wistar rats. Wistar rats were placed into eight groups ($n = 6$) and administered 1 mM/0.5 μ L ICV-OUA injections for three days. Neurochemical assessments were done in rat brain homogenates, CSF, and blood plasma samples at the end of the experiment protocol schedule. Long-term SNL and lithium administration have been shown to decrease the number of rearing and crossings and reduce time spent in the center, locomotor activities, and immobility time. Solanesol treatment gradually raises the amount of Na⁺/K⁺ ATPase, limiting the severity of behavioural symptoms. These findings also revealed that SNL increases the levels of SIRT-1 in CSF, blood plasma, and brain homogenate samples. Moreover, in rat brain homogenates and blood plasma samples, SNL modulates apoptotic markers such as Caspase-3, Bax (pro-apoptotic), and Bcl-2 (anti-apoptotic). Mitochondrial-ETC complex enzymes, including complex-I, II, IV, V, and CoQ10, were also restored following long-term SNL treatment. Furthermore, SNL lowered inflammatory cytokines (TNF- α , IL-1 β) levels while restoring neurotransmitter levels (serotonin, dopamine, glutamate, and acetylcholine) and decreasing oxidative stress markers. Histological examinations also validated Solanesol's protective effect. As a result, our findings suggest that SNL, as a SIRT-1 signalling activator, may be a promising therapeutic approach for BD-like neurological dysfunctions.

Keywords: bipolar disorder; lithium; neuroprotection; ouabain; SIRT-1; solanesol

1. Introduction

Bipolar Disorder is a highly heritable mental condition marked by severe episodes of depression, mania, psychosis, and cognitive impairments [1–3]. It has a complicated origin and is associated with an elevated risk of morbidity, mortality, and comorbidity in psychiatry [4–6]. BD is unique among mental conditions in that its symptoms fluctuate between two distinct mood states: mania and depression [7].

The experimental animal model of mania induced by OUA, a Na⁺/K⁺-ATPase enzyme inhibitor, meets these key characteristics, making it suitable for studying numerous behavioral and neurochemical aspects of BD [8]. OUA dose-dependently increases locomotor activity in rats, which is associated with manic-like behavior [9]. In addition to maintaining Na⁺/K⁺ equilibrium, the Na⁺/K⁺-ATPase is an ion transporter that modulates neuronal excitability, electrochemical gradient, resting membrane potential, and neurotransmitter release and uptake [10–12]. Additionally, ICV injection of OUA into rats results in neurochemical changes comparable to those observed in BD patients, as well as impairments in neurotrophic factors, mitochondrial function, and oxidative stress [13].

SIRT-1 is a protein found in the adult brain and spinal cord, most notably in the amygdala, hippocampus, cerebellum, hypothalamus, and deeper into the neuronal body [14,15]. SIRT-1 protein's deacetylation influences cellular processes such as ageing, inflammation, apoptosis, brain progenitor fates, mitochondrial biogenesis, and stress resistance [16–20].

Dysregulation of SIRT-1 enhances disease progression by increasing oxidative damage and inflammation [21,22]. In a recent study, SIRT-1 activation was shown to increase cell survival, decrease cell apoptosis, and diminish the release of pro-inflammatory cytokines [23]. Hypothalamic circuits have increased SIRT-1 specificity due to changes in SIRT-1 downstream factors such as the transcription factor FoxO. Thus, researchers evaluated the relationship between elevating SIRT-1 protein levels rather than reducing SIRT-1 expression and controlling disease progressions such as obesity, cardiovascular disease, and neurodegeneration [24,25]. SIRT-1 deficiency affects transcription factors (p53, PGC-1, NF- κ B, and FOXO) as well as molecular alterations like gene expression, which influences brain plasticity, Th17 cell suppression, and interleukin-1 production [26,27]. SIRT-1 activation via SIRT-1 activators appears to help with mood disorders [28], MS [29], Parkinson's disease (PD) [30], and Alzheimer's disease (AD) [18]. Recent studies have found a relationship between SIRT-1 deficiency and disease progression and increased oxidative stress and inflammation [31].

In humans, SIRT-1 downregulation has been associated with a depressed phase [32]. According to Abe-Higuchi et al., chronic stress lowers SIRT-1 activity in the dentate gyrus and suppresses the hippocampus SIRT-1 level. Under stressful conditions, activating hippocampus SIRT-1 function was associated with antidepressive behaviors [33]. Another study found that chronic variable stress (CVS) increased depressive-like behavior, which was associated with a decrease in ERK1/2 phosphorylation, Bcl-2 expression, and H4 (K12) acetylation in the hippocampus subregions after chronic stress [34]. SIRT-1 deficiency increased dopamine neurotransmission, resulting in manic-like episodes of bipolar disorder [35].

Solanesol (SNL) is a Solanaceae family crop produced by the 'Nicotiana Tobacco' plant. SNL is a long-chain polyisoprenoid alcohol molecule with nine isoprene units that have also been discovered as a CoQ10 precursor in regulating mitochondrial [36,37]. SNL possesses a variety of pharmacological effects, such as antibacterial, anti-inflammatory, and anti-tumour characteristics. It is utilised in the pharmaceutical industry to manufacture coenzyme Q10, vitamin K2, and N-solanesy1-N, N'-bis(3,4-dimethoxybenzyl) ethylenediamine (SDB) [38]. Several neurodegenerative illnesses that may benefit from SNL treatment include amyotrophic lateral sclerosis (ALS) [39] and multiple sclerosis (MS) [40]. CoQ10

precursors have been demonstrated to protect against migraine [41] and Huntington's disease [42]. CoQ10 precursors have been associated to the prevention of neurodegenerative disorders such as Parkinson's [43] and amyotrophic lateral sclerosis (ALS) [44]. It has also been proven to be useful in the treatment of Alzheimer's disease, multiple sclerosis [45], and bipolar disorder (BD) [46]. It is considered to increase the body's immune system, improve cognitive function, and have anti-oxidant and anti-ageing qualities [47]. CoQ10 has also been demonstrated to protect against IR injury in the liver via activating the SIRT-1 pathway [48]. SNL, as a SIRT-1 signalling activator, has been found to have neuroprotective potential against Alzheimer's disease [49], intracerebral haemorrhage (ICH) [36], and autism [37]. It also has neuroprotective properties against MS [40,50].

On the other hand, hypoactivity alone is insufficient to mimic a depressive state behavior, and additional study is required to support this hypothesis. The "Na⁺/K⁺-ATPase hypothesis", which proposes that decreased enzyme activity is important in developing manic and depressive mood episodes in BD, was used to develop the OUA model of mania [51]. Several investigations have found that the activity of the Na⁺/K⁺-ATPase is diminished in bipolar individuals [52,53]. Lithium's mood-stabilizing therapeutic benefits were identified without any relevant mechanistic information on BD [54]. Current medications, such as lithium alone or in combination, are effective in 60 percent of people regularly treated for manic attacks [55]. Although olanzapine, quetiapine, and ziprasidone [56], valproate, carbamazepine, and lamotrigine [57], some FDA approved drug are generally helpful in reversing manic episodes and avoiding future incidents. They are, however, of little or no value in the acute treatment of depressive episodes. Furthermore, conventional antidepressants, whether given alone or in combination with mood stabilizers or antipsychotics are often ineffective for treating depressive episodes and may promote mood flipping in a group of persons with BD [58].

Thus, in the current study, we have examined the effect of SNL on the levels of SIRT-1 protein in rat brain homogenates, blood plasma, and CSF samples and its neuroprotective potential by evaluating the restoration in the behavioural and neurochemical alterations in OUA-induced BD-like rats through its potential target-modulating properties.

2. Results

2.1. Neuroprotective Potential of Solanesol on Weight Variations in Ouabain-Induced Bipolar Disorder Rats

Improvement in Body Weight after Solanesol Treatment

Bodyweight was measured once a week, on days 1st, 7th, 14th, 21st, and 28th of the procedure schedule. Figure 1 depicts the differences in body weight caused by the toxin OUA compared to the treatment drugs over the protocol schedule. Compared to the vehicle, sham, and SNL80 *per se* treated groups, the administration of OUA for 1st, 3rd, and 7th days resulted in a consistent decline in body weight. From day 8th to day 28th, rats receiving prolonged oral treatment with SNL and Lithium demonstrate a remarkable restoration in body weight due to improvements in psychiatric behaviors such as decreased locomotor activity, rearing, stress, and increased food intake.

Compared to SNL40 and SNL80 mg/kg treated rats, the Li60 mg/kg treated rats showed a more significant improvement in body weight. In addition, compared to other drug treatment groups such as SNL40 mg/kg, SNL80 mg/kg, and Li60 mg/kg, standard drug Li60 mg/kg in combination with SNL80 mg/kg showed significant weight restoration. SNL80 mg/kg is more effective than SNL40 mg/kg in recovering OUA-induced lower body weight, demonstrating that SNL has a dose-dependent impact on restoring body weight [Two-way ANOVA: $F(28, 160) = 903.4, p < 0.001$] (Figure 1).

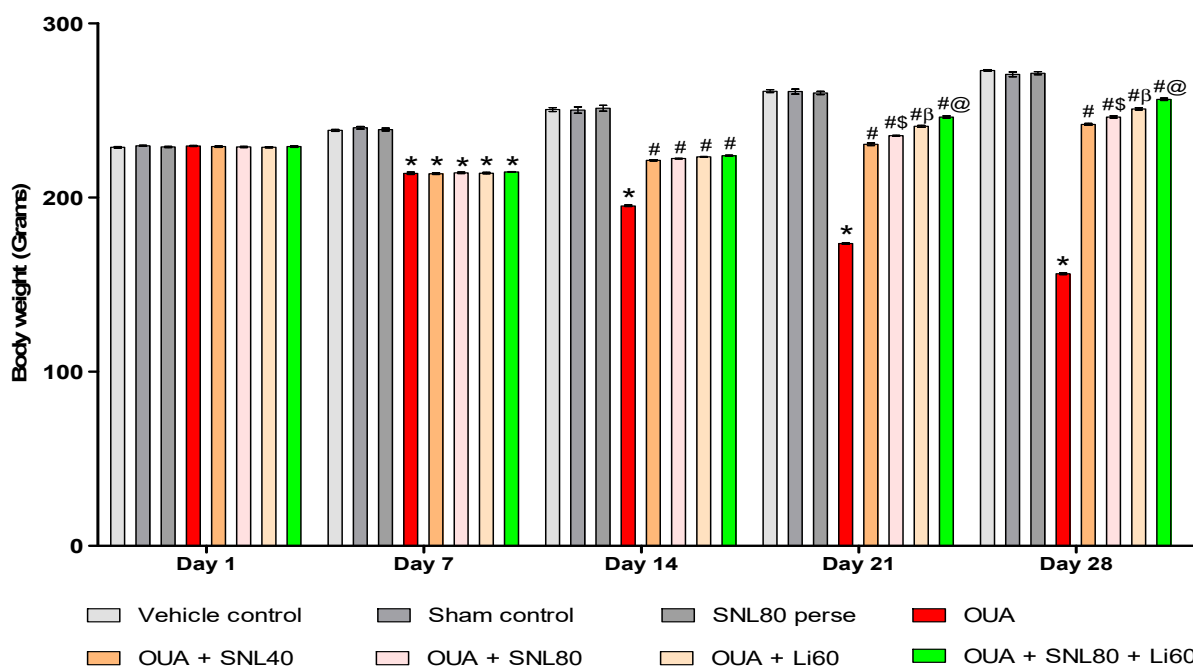


Figure 1. Neuroprotective potential of solanesol on body weight in ouabain-induced bipolar disorder rats. Statistical analysis followed by two-way ANOVA (post-hoc Bonferroni's test). Values are expressed as mean \pm SEM ($n = 6$ rats per group). * $p < 0.001$ v/s vehicle control, sham control and SNL80 *per se*; # $p < 0.001$ v/s OUA; # $\$$ $p < 0.001$ v/s OUA + SNL40; # β $p < 0.001$ v/s OUA + SNL40 and OUA + SNL80; #@ OUA + Li60.

2.2. Neuroprotective Potential of Solanesol in the Prevention of Neurobehavioral Abnormalities in Ouabain-Induced Bipolar Disorder Rats

2.2.1. Decrease Manic-Like Behavior after Solanesol Treatment in the Open Field Task

Three days (1st, 3rd, and 7th) following a single OUA injection, the animals developed manic-like behaviors, as seen by increased crossings, rearings, and time spent in the center. Open field parameters were conducted on days 1st, 7th, 14th, 21st, and 28th of the protocol period to determine the number of crossings, the number of rearings, and time spent in the center in rats.

Decrease Number of Crossing after Solanesol Treatment

The number of boxes crossed by rats in an open field is depicted in Figure 2A. There was no significant difference between the groups on the 1st day. The OUA-treated rats crossed more boxes than the vehicle, sham, and SNL80-treated rats. On the 7th day, there was no significant difference between the OUA-treated group and the other treatment groups. After 20 days of oral administration of the neurotoxic OUA, the SNL treatment group had a progressive reduction in the number of boxes crossing compared to the vehicle control, sham control, and SNL80 *per se* groups on days 14th, 21st, and 28th. On the 21st and 28th days, the Li60 mg/kg alone and combined with SNL80 mg/kg treated animals had considerably reduced the number of boxes crossing than the SNL80 mg/kg and SNL40 mg/kg treated groups. Furthermore, when comparing SNL80 mg/kg treatment to SNL40 mg/kg treatment in BD-like rats, animals showed a lesser number of boxes crossed [Two-way ANOVA: $F(28,160) = 190.0$, $p < 0.001$] (Figure 2A).

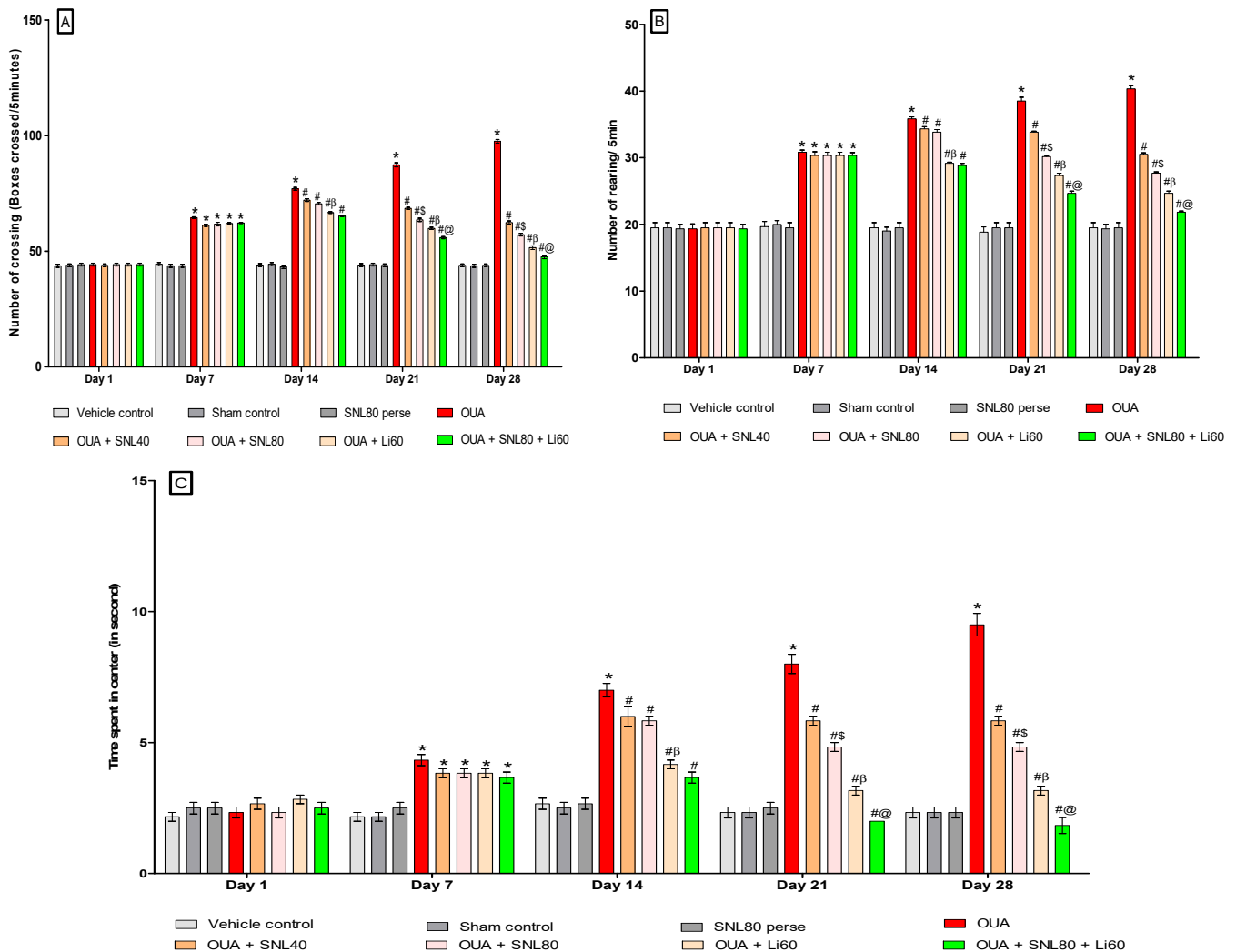


Figure 2. (A) Neuroprotective potential of solanesol on the number of crossing in OUA-induced bipolar disorder rats. Statistical analysis followed by two-way ANOVA (post-hoc Bonferroni's test). Values are expressed as mean \pm SEM ($n = 6$ rats per group). (B) Neuroprotective potential of solanesol on the number of rearing in OUA-induced bipolar disorder rats. Statistical analysis followed by two-way ANOVA (post-hoc Bonferroni's test). (C) Neuroprotective potential of solanesol on time spent in center in OUA induced bipolar disorder rats. Statistical analysis followed by two-way ANOVA (post-hoc Bonferroni's test). * $p < 0.001$ v/s vehicle control, sham control and SNL80 *per se*; # $p < 0.001$ v/s OUA; #\\$ $p < 0.001$ v/s OUA + SNL40; # β $p < 0.001$ v/s OUA + SNL40 and OUA + SNL80; #@ OUA + Li60.

Decrease Number of Rearing after Solanesol Treatment

In the open field, the number of rearing behaviours in BD-like rats is shown in Figure 2B. On the 1st day, there was no significant difference between the groups. The OUA-treated rats showed more rearing moves than the vehicle control, sham control, and SNL80 treated rats. There was no significant difference between the OUA treated and other treatment groups on the 7th day. On days 14th, 21st, and 28th, after 20 days of oral administration of the OUA, the number of rearings in the SNL treated groups decreased over time compared to the vehicle control, sham control, and SNL80 *per se* groups. The Li60 mg/kg alone and Li60 mg/kg along with SNL80 mg/kg treated animals showed a significantly lesser number of rearing on the 21st and 28th days than the SNL80 mg/kg and SNL40 mg/kg treated groups. Furthermore, when BD-like rats were

given SNL80 mg/kg versus SNL40 mg/kg, the animals showed a lesser number of rearing movements. [Two-way ANOVA: $F(28,160) = 39.51, p < 0.001$] (Figure 2B).

Decrease Time Spent in the Centre after Solanesol Treatment

Figure 2C indicates BD-like rats in the open field time spent in the centre. On the 1st day, there was no significant difference between the groups. The OUA-treated rats stayed longer than vehicle, sham, and SNL80-treated rats. There was no significant difference between the OUA-treated group and the other treatment groups on the seventh day. On days 14th, 21st, and 28th compared to the vehicle control, sham control, and SNL80 *per se* groups, time spent in the center in the SNL treated groups reduced over time following 20 days of oral administration of the OUA. The Li60 mg/kg alone and Li60 mg/kg combined with SNL80 mg/kg treated animals spent significantly less time in the centre on the 21st and 28th days than the SNL80 mg/kg and SNL40 mg/kg treated groups. Moreover, BD-like rats administered SNL80 mg/kg spent less time in the center than rats given SNL40 mg/kg. [Two-way ANOVA: $F(28,160) = 27.00, p < 0.001$] (Figure 2C).

2.2.2. Decreased Manic-Like Behavior after Solanesol Treatment

As illustrated in Figure 3, the results suggest that OUA significantly affects locomotor activity in BD-like rats. On the 1st day, there was no significant difference between the groups. Rats were given OUA on days 1st, 3rd, and 7th, demonstrating considerably higher locomotor activity during the protocol schedule than the vehicle control, sham control, and SNL80 treated rats. Locomotor activity decreased from day 8th to day 28th after SNL treatment, as observed with the mood stabilizer Li60 mg/kg treated rats. Compared to the SNL80 mg/kg and SNL40 mg/kg treatment groups, Li60 mg/kg administration, both alone and in combination with SNL80 mg/kg, significantly reduced locomotor activity. In addition, SNL80 mg/kg significantly reduced locomotor activity in actophotometer rats when compared to SNL40 mg/kg treated rats on day 27th [Two-way ANOVA: $F(21,120) = 244.1, p < 0.001$]. These results indicate that Lithium and SNL have an antimanic effect when given alone and a more significant enhancement in antimanic action when given together during OUA-induced BD like rats on days 18th and 27th (Figure 3).

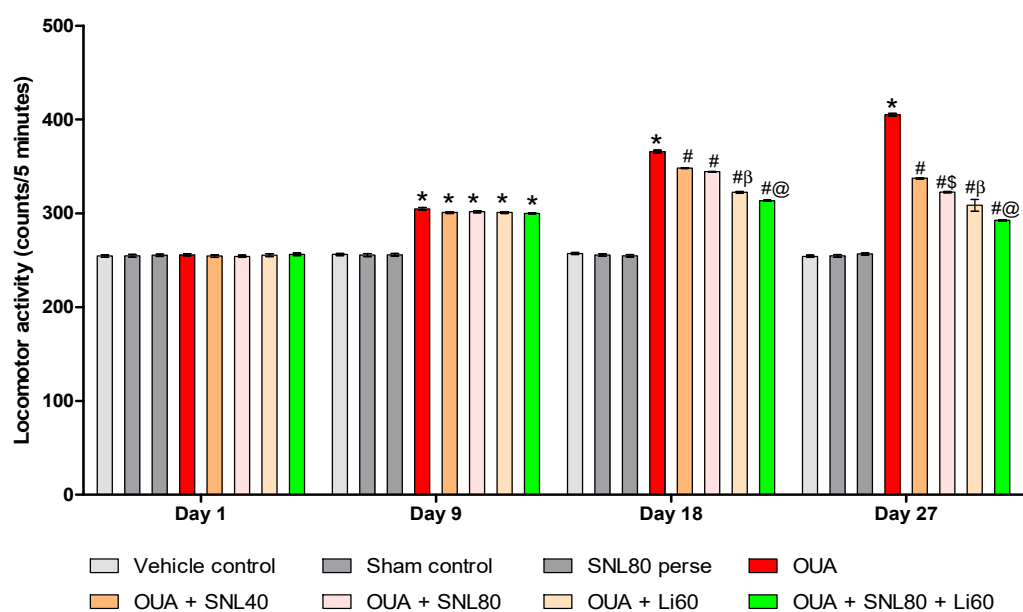


Figure 3. Neuroprotective potential of solanesol on locomotor activity in OUA-induced bipolar disorder rats. Statistical analysis followed by two-way ANOVA (post-hoc Bonferroni's test). Values expressed as mean \pm SEM ($n = 6$ rats per group). * $p < 0.001$ v/s vehicle control, sham control and SNL80 *per se*; # $p < 0.001$ v/s OUA; # β $p < 0.001$ v/s OUA + SNL40; # β $p < 0.001$ v/s OUA + SNL80; #@ $p < 0.001$ v/s OUA + Li60.

2.2.3. Decreased Depression-Like Behavior after Solanesol Treatment

As shown in Figure 4, the results reveal that OUA considerably influences immobility time in BD-like rats. On the 1st day, there was no significant difference between the groups. Rats were given OUA on days 1st, 3rd, and 7th and had significantly prolonged immobility time during the protocol schedule compared to the vehicle control, sham control, and SNL80 *per se* treated rats. From day 8th to day 28th, immobility time was significantly reduced with SNL treatment, as reported with the mood stabilizer Li60 mg/kg. Li60 mg/kg treatment, combined with SNL80 mg/kg, significantly reduced immobility time compared to the SNL80 mg/kg and SNL40 mg/kg treatment groups. Furthermore, compared to SNL40 mg/kg treated rats on day 27th, SNL80 mg/kg significantly reduced immobility time in FST rats [Two-way ANOVA: $F(21,120) = 244.1$, $p < 0.001$] Li60 mg/kg and SNL80 mg/kg showed an antidepressant effect when administered alone on day 27th in OUA-induced BD like rats and a more significant effect when given in combination (Figure 4).

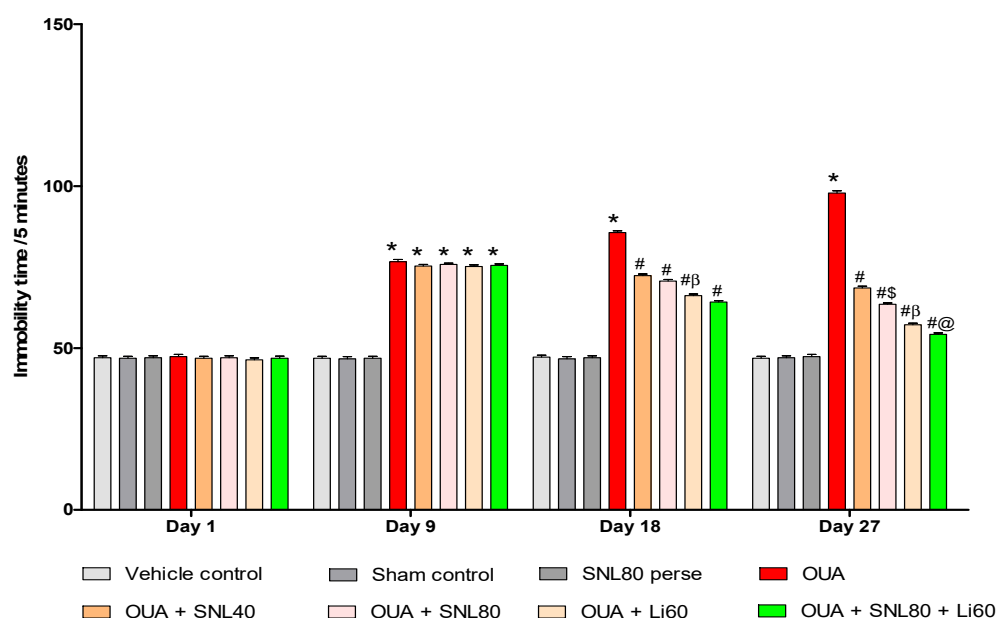


Figure 4. Neuroprotective potential of solanesol on immobility time in OUA-induced bipolar disorder rats. Statistical analysis followed by two-way ANOVA (post-hoc Bonferroni's test). Values expressed as mean \pm SEM ($n = 6$ rats per group). * $p < 0.001$ v/s vehicle control, sham control and SNL80 *per se*; # $p < 0.001$ v/s OUA; # β $p < 0.001$ v/s OUA + SNL40; # β $p < 0.001$ v/s OUA + SNL40 and OUA + SNL80; #@ OUA + Li60.

2.3. Neuroprotective Potential of Solanesol on Neurochemical Alterations in Ouabain-Induced Bipolar Disorder Rats

2.3.1. Increased SIRT-1 Level after Long-Term Administration of Solanesol

At the end of the protocol schedule, SIRT-1 levels were measured in rat brain homogenate, blood plasma, and CSF samples. Compared to vehicle control, sham control, and SNL80 *per se* groups, the ICV injection of OUA significantly declined SIRT-1 levels. The level of SIRT-1 in brain homogenate [One-way ANOVA: $F(7,35) = 4.472$, $p < 0.001$], blood plasma [One-way ANOVA: $F(7,35) = 5.938$, $p < 0.001$], and CSF [One-way ANOVA: $F(7,35) = 1.243$, $p < 0.001$] samples were elevated after continuous oral administration of SNL at doses of 40 mg/kg and 80 mg/kg. In rat brain homogenate, blood plasma, and CSF samples, SNL80 mg/kg was more effective than SNL40 mg/kg in restoring SIRT-1 protein expression. Furthermore, the Li60 mg/kg alone and Li60 mg/kg combined with SNL80 mg/kg treated groups were more effective in restoring SIRT-1 protein expression in rat brain homogenate, blood plasma, and CSF samples than the SNL80 mg/kg and SNL40 mg/kg treated groups (Figure 5A–C).

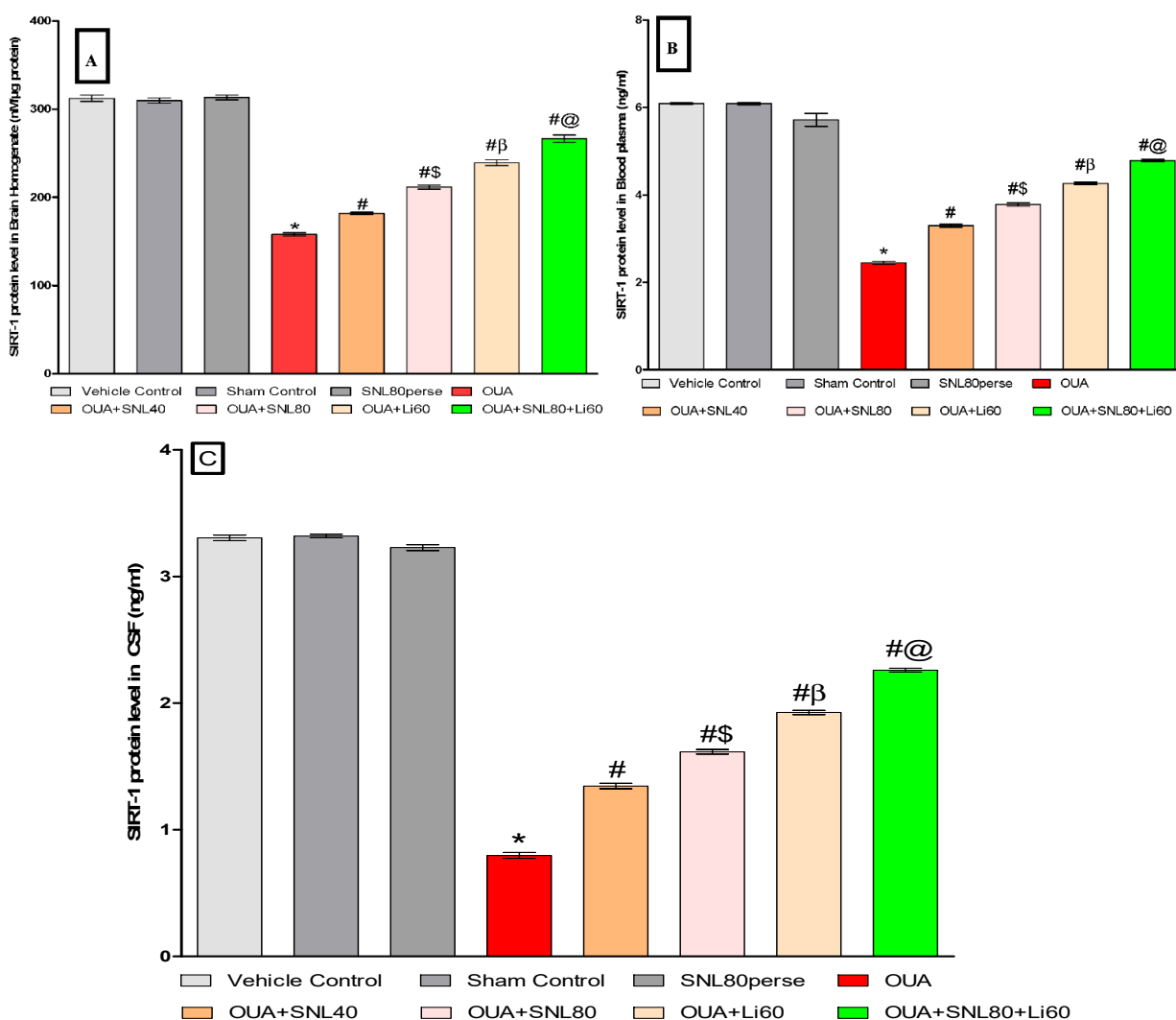


Figure 5. Neuroprotective potential of solanesol on SIRT-1 level in ouabain-induced bipolar disorder in rats (A–C). Statistical analysis followed by one-way ANOVA (post-hoc tukey test). Values expressed as mean \pm SEM ($n = 6$ rats per group). * $p < 0.001$ v/s vehicle control, sham control and SNL80 *per se*; # $p < 0.001$ v/s OUA; # β $p < 0.001$ v/s OUA + SNL40; # β $p < 0.001$ v/s OUA + SNL40 and OUA + SNL80; #@ OUA + Li60.

2.3.2. Decreased Level of Caspase-3, Bax, and Increased Bcl-2 Levels after Long-Term Administration of Solanesol

The levels of cell death indicators such as Caspase-3, Bax, and Bcl-2 were measured in rat brain homogenate and blood plasma samples after the protocol schedule. In rat brain homogenate and blood plasma samples, ICV injection of OUA treatment resulted in a significant increase in pro-apoptotic markers such as caspase-3 and Bax. In contrast, the ICV injection of OUA for three days (1st, 3rd, and 7th) resulted in a significant decrease in anti-apoptotic Bcl-2 protein levels in rat brain homogenate and blood plasma samples compared to the vehicle control, sham control, and SNL80 *per se* treated groups. Chronic oral treatment of SNL40 mg/kg and SNL80 mg/kg significantly lowered caspase-3 levels in brain homogenate [One-way ANOVA: $F(7, 35) = 0.522$, $p < 0.001$] and blood plasma samples [One-way ANOVA: $F(7, 35) = 1.739$, $p < 0.001$] respectively.

Similarly, continuous oral administration of SNL40 mg/kg and 80 mg/kg significantly reduced the amount of pro-apoptotic Bax in rat brain homogenate [One-way ANOVA: $F(7, 35) = 1.092$, $p < 0.001$] and blood plasma samples [One-way ANOVA: $F(7, 35) = 1.628$, $p < 0.001$].

Furthermore, regular oral administration of SNL at doses of 40 mg/kg and 80 mg/kg for 20 days (day 8th to 28th) resulted in a significant rise in Bcl-2 protein levels in brain homogenate [One-way ANOVA: $F(7, 35) = 1.325, p < 0.001$] and blood plasma [One-way ANOVA: $F(7, 35) = 1.968, p < 0.001$] samples to the OUA-treated BD like rats. Also, SNL80 mg/kg treatment was more effective than SNL40 mg/kg treatment in restoring abnormal levels of apoptotic markers in BD-like rats. Furthermore, in rat brain homogenate and blood plasma, the Li60 mg/kg alone and Li60 mg/kg combined with SNL80 mg/kg treated groups showed more significance in restoring the altered levels of apoptotic markers than the SNL80 mg/kg and SNL40 mg/kg treated groups (Figure 6A–F).

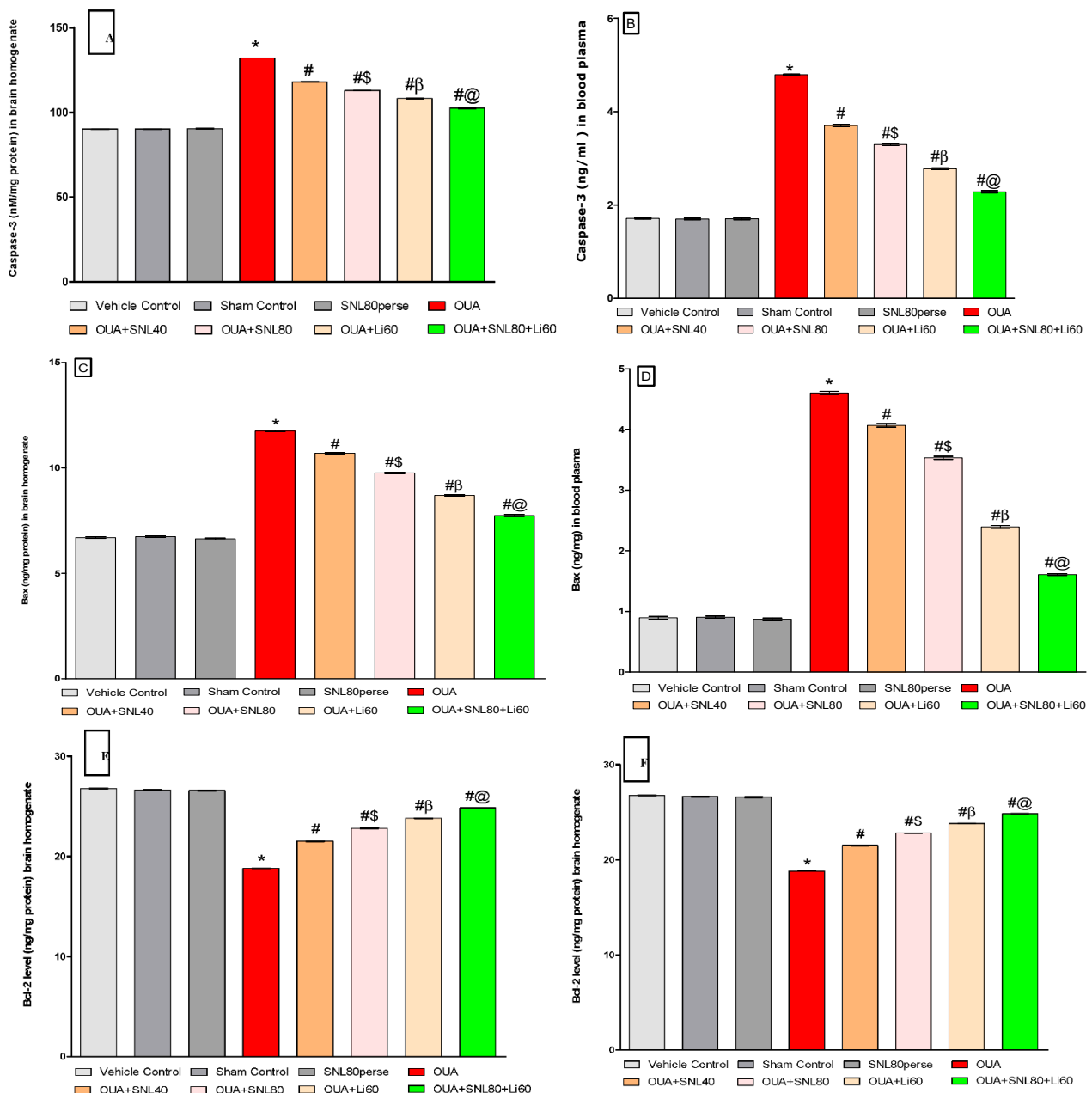


Figure 6. Neuroprotective potential of solanesol on Caspase-3, Bax, and Bcl-2 level in ouabain-induced bipolar disorder in rats (A–F). Statistical analysis followed by one-way ANOVA (post-hoc Tukey's test). Values expressed as mean \pm SEM ($n = 6$ rats per group). * $p < 0.001$ v/s vehicle control, sham control and SNL80 per se; # $p < 0.001$ v/s OUA; # $\$$ $p < 0.001$ v/s OUA + SNL40; # β $p < 0.001$ v/s OUA + SNL40 and OUA + SNL80; #@ OUA + Li60.

2.3.3. Restoration of Mitochondrial ETC-Complexes Enzyme Level after Long-Term Administration of Solanesol

After the experiment protocol schedule, the enzyme activity of mitochondrial ETC-complexes was evaluated in rat brain homogenate. Three days of intoxications of OUA in rats through ICV injection resulted in a significant decrease in mitochondrial ETC complexes-I [One-way ANOVA: $F(7, 35) = 1.796, p < 0.001$], complexes-II [One-way ANOVA: $F(7, 35) = 2.936, p < 0.001$], complexes-IV [One-way ANOVA: $F(7, 35) = 6.744, p < 0.001$], and complexes-V [One-way ANOVA: $F(7, 35) = 0.979, p < 0.001$] and CoQ10 level [One-way ANOVA: $F(7, 35) = 4.381, p < 0.001$], when compared to the vehicle, sham control, and SNL80 *per se* groups.

In OUA-treated rats, twenty days of chronic administration with SNL40mg/kg and SNL80 mg/kg substantially and dose-dependently recovers and increases mitochondrial ETC complex enzymatic activity. The significant restoration was observed with a high dose of SNL80 mg/kg group in mitochondrial ETC complexes-I, II, IV, V, and CoQ10 compared to a low dose of SNL40 mg/kg. The most significant improvements in mitochondrial ETC complexes-I, II, IV, V, and CoQ10 in rat brain homogenate were seen in the Li60 mg/kg alone and Li60 mg/kg in combination with SNL80 mg/kg treated groups, which were more effective than the SNL80 mg/kg and SNL40 mg/kg treated groups (Figure 7A–E).

2.3.4. Restoration of Neurotransmitter Level after Long-Term Administration of Solanesol

Neurochemicals such as serotonin, dopamine, glutamate, and acetylcholine were analyzed in rat brain homogenate samples at the end of the experimental protocol schedule. The injection of OUA through the ICV route considerably reduced serotonin and acetylcholine levels. ICV injection of OUA intoxication resulted in a significant increase in dopamine and glutamate concentrations in brain homogenate compared to vehicle control, sham control, and SNL80 *per se* treated rats. Treatment with SNL40 mg/kg and 80 mg/kg significantly and dose-dependently increased serotonin [One-way ANOVA: $F(7,35) = 4.031, p < 0.001$] as well as acetylcholine level [One-way ANOVA: $F(7,35) = 3.607, p < 0.001$]. In contrast to the OUA-treated BD-like rats, prolonged oral administration of SNL40 mg/kg and SNL80 mg/kg decreased the concentrations of dopamine [One-way ANOVA: $F(7,35) = 1.000, p < 0.001$] and glutamate [One-way ANOVA: $F(7,35) = 1.963, p < 0.001$] in rat brain homogenate. Moreover, SNL80 mg/kg versus SNL40 mg/kg treated rats re-establish lower neurotransmitter levels. The Li60 mg/kg alone and Li60 mg/kg combined with SNL80 mg/kg treated groups were more effective than the SNL80 mg/kg, and SNL40 mg/kg treated groups in restoring the altered levels of neurotransmitters in rat brain homogenate (Figure 8A–D).

2.3.5. Reduction in Neuroinflammatory Cytokines after Long-Term Administration of Solanesol

We measured the levels of pro-inflammatory cytokines like TNF- α and IL-1 β in the whole brain homogenate and blood plasma samples of rats to see whether SNL had a therapeutic effect in OUA-induced BD-like rats. SNL therapy at doses of 40 mg/kg and 80 mg/kg reduced TNF- α expression in rat brain homogenate [One-way ANOVA: $F(7, 35) = 1.065, p < 0.001$] and blood plasma samples [One-way ANOVA: $F(7, 35) = 0.589, p < 0.001$]. Similarly, chronic oral treatment with SNL40 mg/kg and SNL80 mg/kg remarkably decreased the level of IL-1 β in brain homogenate [One-way ANOVA: $F(7, 35) = 0.348, p < 0.001$] and blood plasma samples [One-way ANOVA: $F(7, 35) = 0.691, p < 0.001$], as opposed to the OUA toxin administered BD like rats. Meanwhile, compared to the SNL40 mg/kg dose, SNL80 mg/kg demonstrated a significant improvement in lowering the expression of these inflammatory mediators. In rat brain homogenate and blood plasma samples, the Li60 mg/kg alone and Li60 mg/kg in conjunction with SNL80 mg/kg treated groups exhibited a substantial improvement in lowering the level of these inflammatory mediators compared to the SNL80 mg/kg, and SNL40 mg/kg treated groups at the end of protocol schedule (Figure 9A–D).

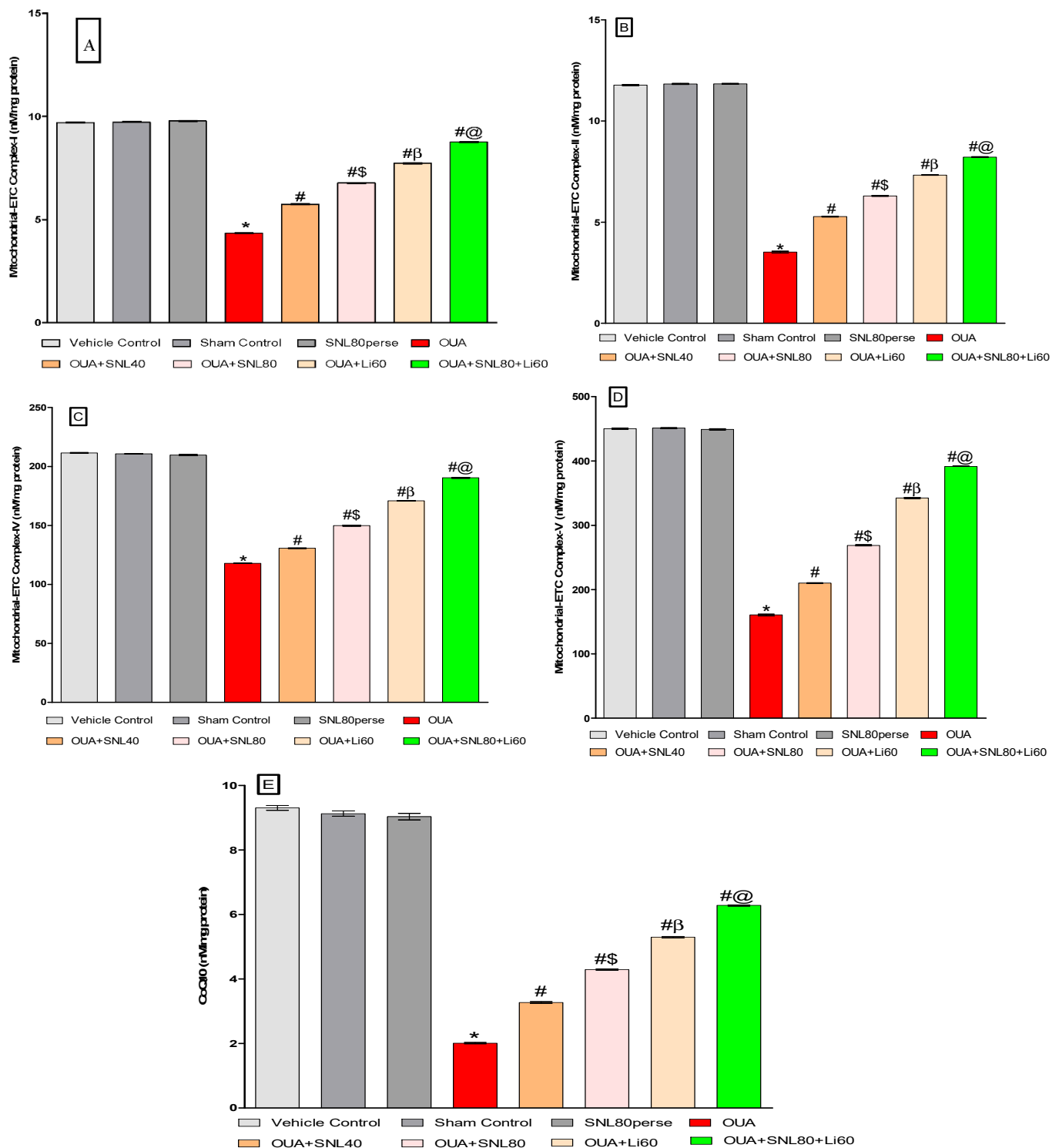


Figure 7. Neuroprotective potential of solanesol in restoration of mitochondrial ETC complex enzymes in ouabain-induced bipolar disorder in rats (A–E). Statistical analysis followed by one-way ANOVA (post-hoc Tukey’s test). Values expressed as mean \pm SEM ($n = 6$ rats per group). * $p < 0.001$ v/s vehicle control, sham control and SNL80 *per se*; # $p < 0.001$ v/s OUA; #\\$ $p < 0.001$ v/s OUA + SNL40; #\beta $p < 0.001$ v/s OUA + SNL40 and OUA + SNL80; #@ OUA + Li60.

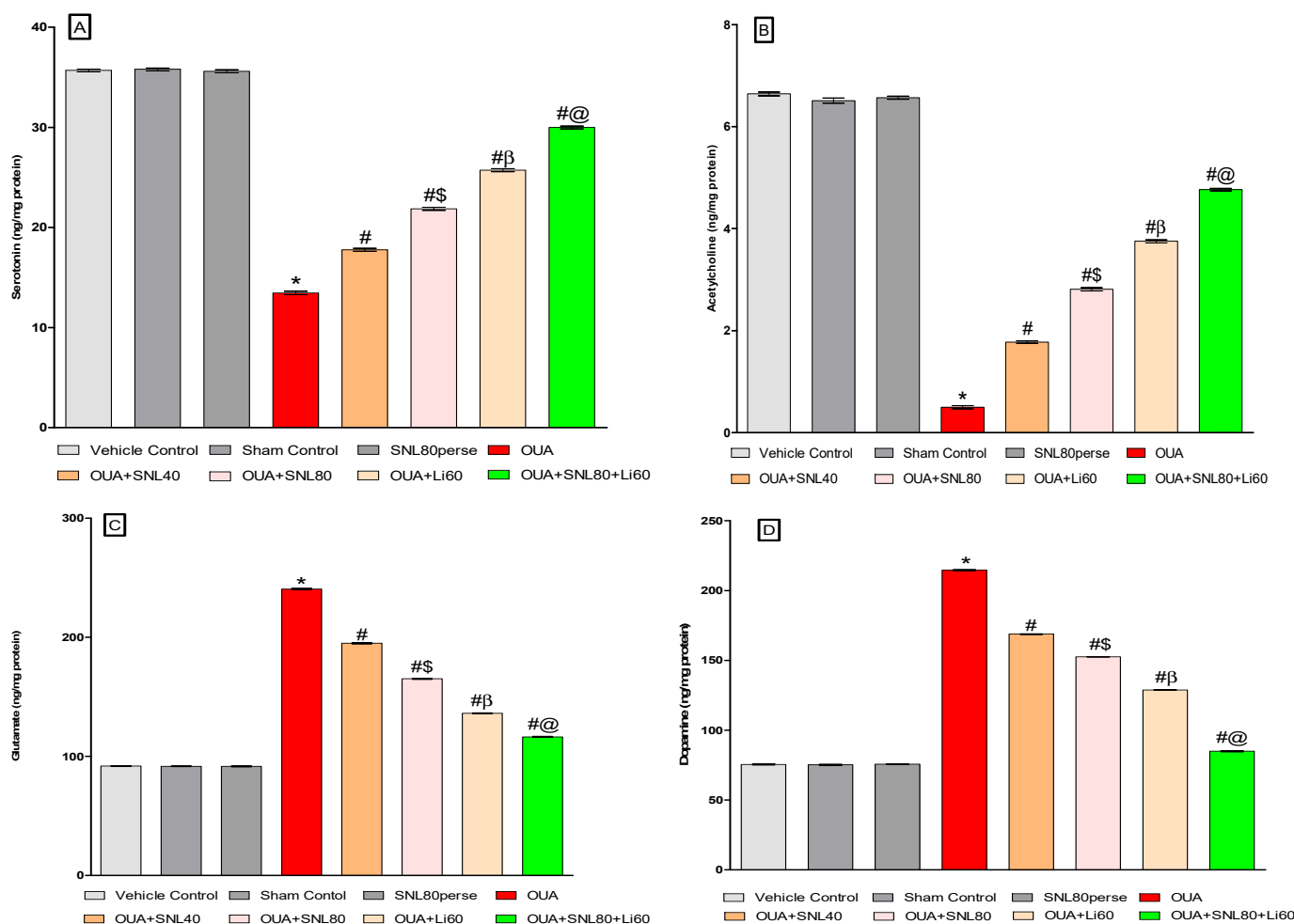


Figure 8. Neuroprotective potential of solanesol on neurotransmitters level in ouabain-induced bipolar disorder in rats (A–D). Statistical analysis followed by one-way ANOVA (post-hoc Tukey’s test). Values expressed as mean \pm SEM ($n = 6$ rats per group). * $p < 0.001$ v/s vehicle control, sham control and SNL80 *per se*; # $p < 0.001$ v/s OUA; # β $p < 0.001$ v/s OUA + SNL40; # β $p < 0.001$ v/s OUA + SNL40 and OUA + SNL80; #@ OUA + Li60.

2.3.6. Decreased Oxidative Stress Markers and Increased Antioxidant Levels after Long-Term Administration of Solanesol

The oxidative stress indicators such as MDA, Nitrite, SOD, GSH and, AChE, LDH were measured in rat brain homogenate samples at the end of the experimental protocol schedule. The levels of MDA, Nitrite, and AChE, LDH increased significantly after ICV injection of OUA. In contrast, antioxidant levels such as SOD and GSH decreased compared to the vehicle control, sham control, and SNL80 *per se* treated groups. Continuous oral treatment of SNL at doses of 40 mg/kg and 80 mg/kg for twenty days significantly lowered the levels of AChE [One-way ANOVA: $F(7,35) = 2.867$, $p < 0.001$], LDH [One-way ANOVA: $F(7,35) = 2.829$, $p < 0.001$], MDA [One-way ANOVA: $F(7,35) = 3.681$, $p < 0.001$] and nitrite [One-way ANOVA: $F(7,35) = 1.736$, $p < 0.001$].

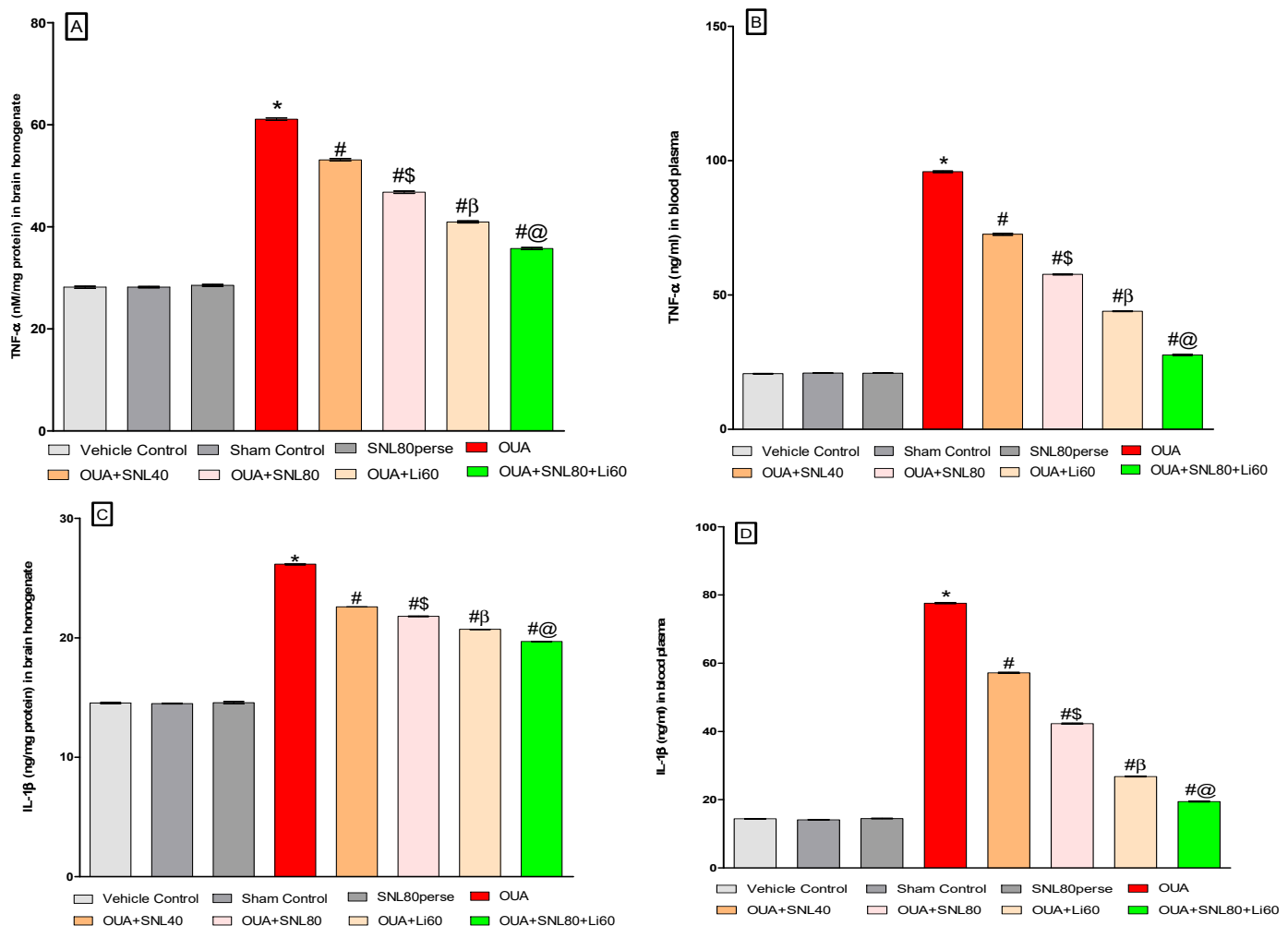


Figure 9. Neuroprotective potential of solanesol on neuroinflammatory cytokines levels in ouabain-induced bipolar disorder in rats (A–D). Statistical analysis followed by one-way ANOVA (post-hoc Tukey’s test). Values expressed as mean \pm SEM ($n = 6$ rats per group). * $p < 0.001$ v/s vehicle control, sham control and SNL80 *per se*; # $p < 0.001$ v/s OUA; # β $p < 0.001$ v/s OUA + SNL40; # β $p < 0.001$ v/s OUA + SNL40 and OUA + SNL80; #@ OUA + Li60.

However, SNL40 mg/kg and SNL80 mg/kg remarkably restored the anti-oxidant defence system by increasing the levels of GSH [One-way ANOVA: $F(7,35) = 4.281$, $p < 0.001$] and SOD [One-way ANOVA: $F(7,35) = 6.111$, $p < 0.001$] when compared with OUA-treated BD like rats. Furthermore, compared to SNL40 mg/kg, SNL80 mg/kg significantly reduced oxidative stress markers and restored antioxidant expression in a dose-dependent manner. Among these, the most significant improvements were observed in the Li60 mg/kg alone and Li60 mg/kg in combination with SNL80 mg/kg treated groups, which were more effective than the SNL80 mg/kg and SNL40 mg/kg treated groups in significantly reducing oxidative stress markers and restoring antioxidant expression (Figure 10A–F).

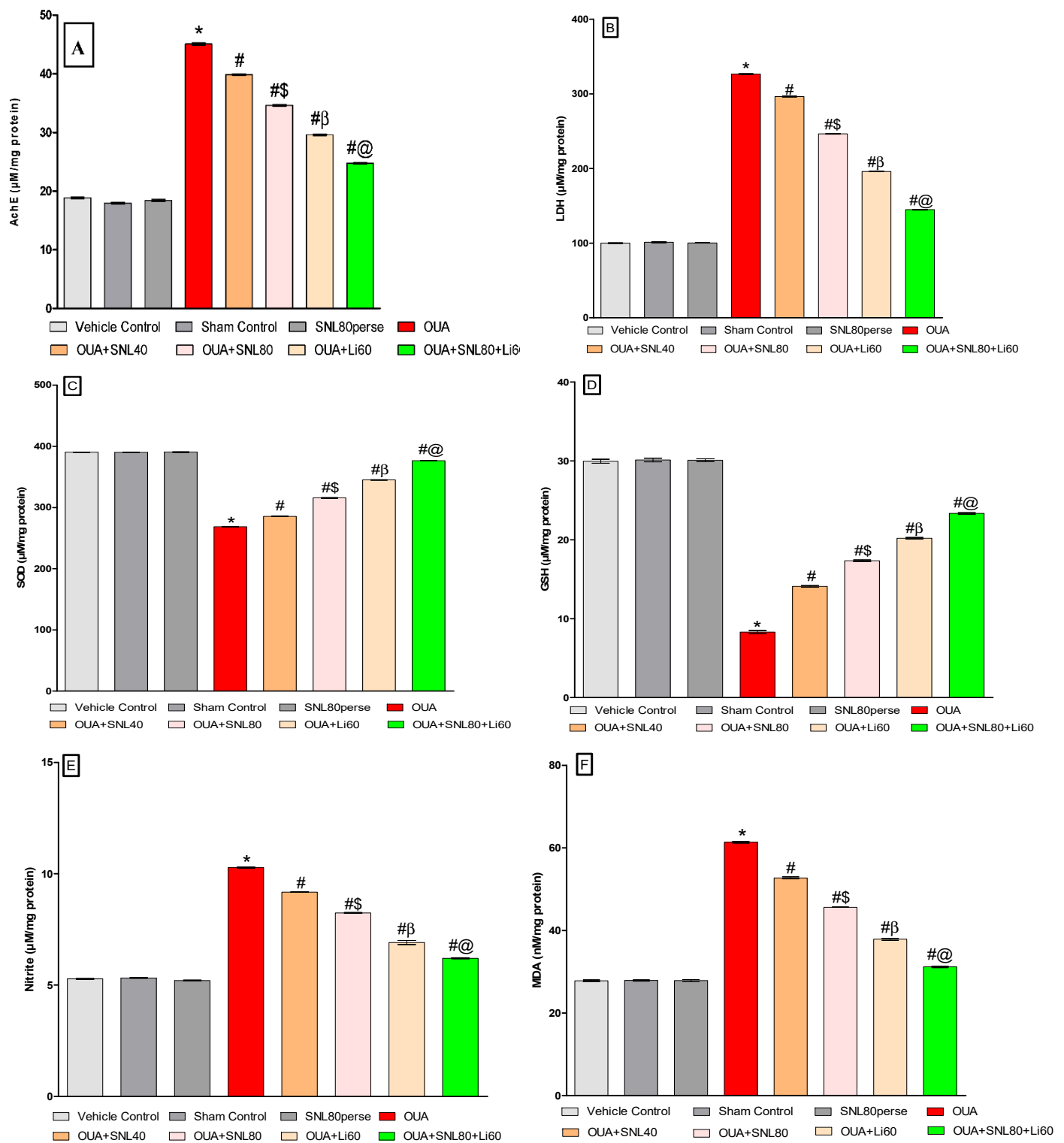


Figure 10. Neuroprotective potential of solanesol on oxidative stress markers level in ouabain-induced bipolar disorder in rats (A–F). Statistical analysis followed by one-way ANOVA (post-hoc Tukey’s test). Values expressed as mean \pm SEM ($n = 6$ rats per group). * $p < 0.001$ v/s vehiclecontrol, sham control and SNL80 *per se*; # $p < 0.001$ v/s OUA; #\\$ $p < 0.001$ v/s OUA + SNL40; # β $p < 0.001$ v/s OUA + SNL40 and OUA + SNL80; #@ OUA + Li60.

2.3.7. Increased Na⁺/K⁺ ATPase Enzyme Activity after Long-Term Administration of Solanesol

The enzyme activity of Na⁺/K⁺ ATPase in rat brain homogenate was assessed immediately afterwards the experiment protocol schedule. Compared to the vehicle control, sham control, and SNL80 *per se* groups, ICV injection of OUA resulted in a substantial decrease in Na⁺/K⁺ ATPase activity. The activity of Na⁺/K⁺ ATPase in rat brain homogenate was increased after continuous oral administration of SNL at dosages of 40 mg/kg and 80 mg/kg [One-way ANOVA: $F(7,35) = 2.236, p < 0.001$]. SNL80 mg/kg restored Na⁺/K⁺ ATPase activity more effectively than SNL40 mg/kg in rat brain homogenate. Furthermore, the Li60 mg/kg alone and combined with SNL80 mg/kg treated groups restored Na⁺/K⁺ ATPase more efficiently than the SNL80 mg/kg and SNL40 mg/kg treated groups (Figure 11).

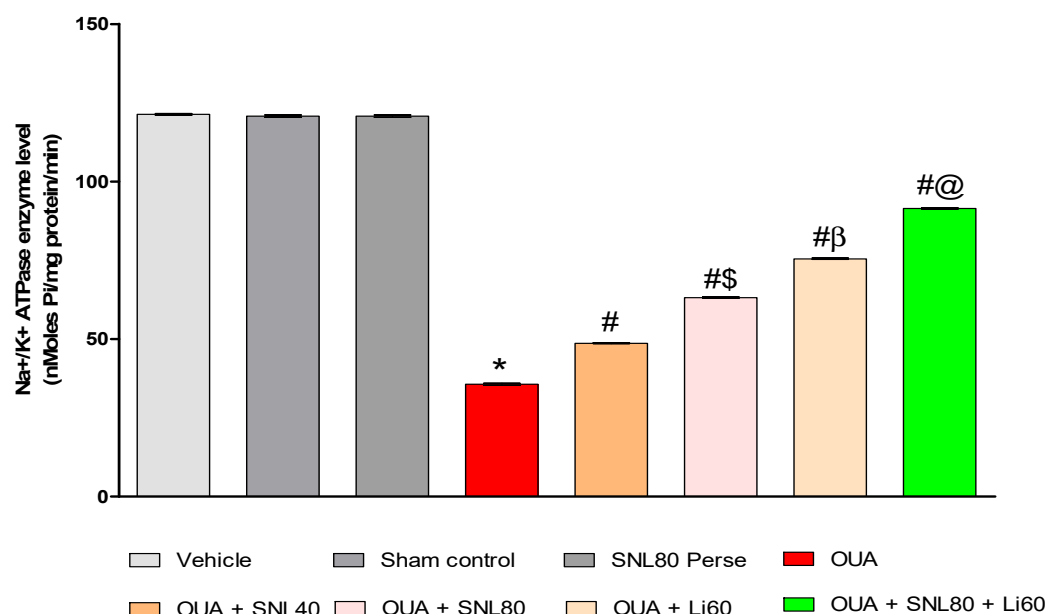


Figure 11. Neuroprotective potential of solanesol on Na⁺/K⁺ ATPase enzyme level in OUA-induced bipolar disorder rats. Statistical analysis followed by one-way ANOVA (post-hoc tukey test). Values expressed as mean ± SEM ($n = 6$ rats per group). * $p < 0.001$ v/s vehicle control, sham control and SNL80 *per se*; # $p < 0.001$ v/s OUA; #\\$ $p < 0.001$ v/s OUA + SNL40; #β $p < 0.001$ v/s OUA + SNL40 and OUA + SNL80; #@ OUA + Li60.

2.4. Neuroprotective Potential of Solanesol on Histopathological Alterations in Ouabain-Induced Bipolar Disorder Rats

The histological evaluation of the striatum revealed no alteration in the vehicle, sham and the SNL *per se* group. Ouabain intoxication increased the number of neuroglial cells, a change in the neuron's shape, and increased apoptosis, thus increasing the damaged area. The SNL treatment reversed the OUA-induced alterations in a dose-dependent manner. Still, Li treatment showed more improvement than the SNL alone, showing a decrease in apoptosis, reduction in the neuroglial cells, and improvement in the neuronal cell structure. However, when a high dose of SNL was given along with the Li showed a remarkable decrease in the neuroglial cell, restoration in the neuronal cell structure, and subsequent reduction in apoptosis (Figure 12).

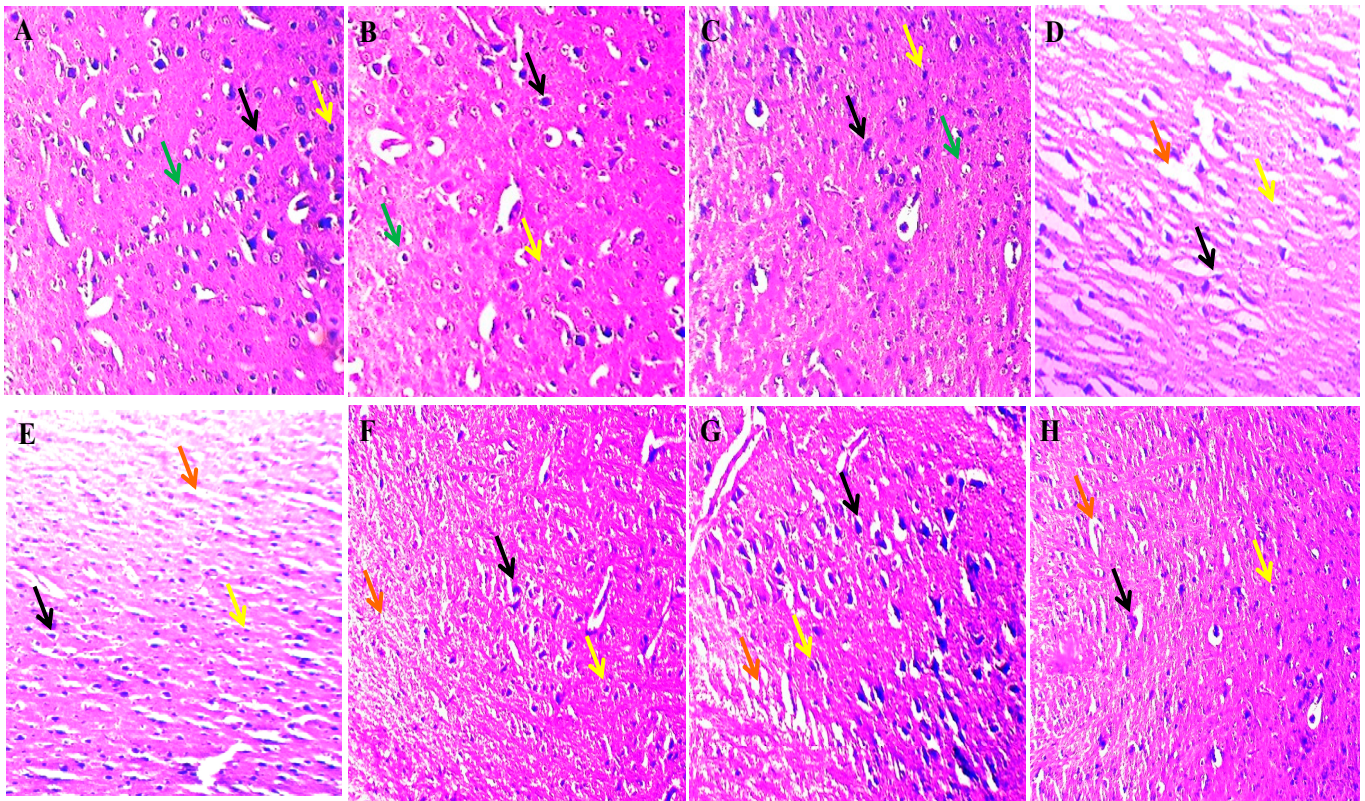


Figure 12. The effect of solanesol on histopathological alterations in ouabain-induced bipolar disorder rats. Histological evaluation via Hematoxylin and eosin staining revealed that in the vehicle (A), sham control (B) and SNL *per se* (C) group, the black arrow represents the typical normal nuclei, the yellow arrow represents the neuroglial cells, and the green arrow represents the oligodendrocytes. The OUA (D) group showed a high damaged area represented by the orange arrow, the black arrow represents abnormal neuronal structure, and the yellow arrow indicates the high neuroglial cell penetration. The SNL showed a dose-dependent improvement in the OUA + SNL40 (E) and 80 (F) group in the histological alteration as the decrease in the damaged area indicated by the orange arrow, slight restoration of abnormal neuronal structure and the yellow arrow represents the mild decrease in the penetration of the neuroglial cell. In the OUA + Li60 (G) group, there was a subsequent reduction in the neuroglial cell penetration as well as the damaged area and the neuronal cells structure restoration indicated by the yellow, orange and black arrows, respectively. The OUA + Li60 + SNL80 (combination group) (H) showed restoration of the neuron cell structure (black arrow), a remarkable decrease in the white area (damaged area) indicated by the orange arrow and a small number of neuroglial cells indicated by the yellow arrow.

3. Discussion

Over the last decade, sirtuins' significance in brain ageing, neurodegenerative disorders including AD, PD, MS, ALS, and neuropsychiatric disorders like BD has been better understood [59–62]. SIRT1's role in Parkinson's, Huntington's, and multiple sclerosis [40] remained unknown until recently. SIRT-1 activity and expression may be a therapeutic target for AD. Activating SIRT-1 reduces behavioural impairment, neurochemical changes, and neuronal damage [63–65]. SIRT-1 activation is connected to synaptic dysfunction, aberrant neurotransmitter release, and genetic variants [66]. No pharmacological animal model can mimic mania and depression in the same animals, according to a study [67]. Valvassori et al. used a single ICV injection of OUA to induce manic and depressive-like behaviour [60].

Several studies have revealed that rats exhibit manic behaviours after ICV injection of OUA [13,68]. After seven days of protocol schedule in ICV-OUA generated BD-like

rats, locomotor activity, number of boxes traversed, number of rearing movements, and time spent at the centre increased significantly. The same animal exhibited manic and depressive-like behaviours after OUA treatment. This work intends to prove that SNL can prevent OUA-induced BD in rats by increasing SIRT-1 protein levels.

In the open field test, forced swimming, or locomotor activity, rats treated with OUA did not differ from vehicle control, sham control, or SNL80 *per se* groups. Nine days following OUA injection, rats may experience calm [60,69,70]. Variation between experiments may be due to rat strains and experimental settings. In the current investigation, biochemical analysis was repeated, and open-field test findings were identical [71].

Several studies suggest lithium can reduce manic-like behaviour in OUA-ICV-injected rats [8,72]. Lithium reversed immobility time. Previous preclinical research showed lithium's antidepressant characteristics [73,74]. However, the current study duplicated depression and manic-like behaviours in a BD animal model.

Developing an animal model of BD utilising OUA is based on the idea that decreased Na^+/K^+ ATPase activity is necessary for commencing manic and depressed mood episodes [60,75]. OUA decreases Na^+/K^+ ATPase activity 7 and 9 days after ICV injection. Na^+/K^+ ATPase's participation in BD was proposed more than 50 years ago [76]. A meta-analysis indicated that BD erythrocytes had decreased Na^+/K^+ ATPase activity [77]. Even a minor reduction in this enzyme activity can increase neuronal excitability and delay Ca^{2+} depuration [78]. Increased neuronal excitability may cause bipolar manic hyperactivity. Long-term Na^+/K^+ -ATPase suppression may impair resting potential control, making neuronal depolarization more difficult. These events may slow neuronal transmission and synaptic effectiveness, causing BD depressive episodes [79]. Lithium may fight oxidation by increasing Na^+/K^+ ATPase activity. Rats with OUA-induced oxidative damage have BD-like pathophysiology. In mania and depression animal models, glutathione enzymes are decreased [80]. Modulating anti-oxidant enzymes is one of lithium's probable therapeutic effects [81]. According to research, reduced Na^+/K^+ ATPase activity in BD patients may be linked to increased dopamine and glutamate neurotransmitter synthesis and oxidative damage [82].

Lithium, a mood stabiliser, can lessen BD symptoms by counteracting pathological alterations. The proposed OUA model could be utilised to study pathophysiology and assess mood stabilisers. Chronic OUA therapy of the brain decreased ATP production, increased oxidative stress mediated by ROS and RNS, and lowered SIRT-1 protein level [60]. SIRT-1 deacetylation modulates its levels in mitochondria and other brain regions. SIRT-1 dysregulation induces memory impairment, and oxidative indicators indicate high ROS and RNS in the brain [83]. In bipolar individuals, oxidative stress reduces Na^+/K^+ ATPase activity [84].

According to current findings, OUA-treated rats had lower body weight on days 14th, 21st, and 28th. Furthermore, on days 9th, 18th, and 27th, there was an increase in locomotor activity in the actophotometer, which was responsible for manic-like behaviour. This manic-like activity was seen by OFT on the 7th, 14th, 21st, and 28th days, demonstrating a progressive rise in the number of rearing, the number of boxes crossing, and time spent in the center. FST on the 9th, 18th, and 27th days indicated an increase in immobility time.

This study investigates the effect of OUA on the protein level of SIRT-1 in the brain, which was found to be lower in brain homogenate, blood plasma, and CSF samples. In addition, the levels of the apoptotic markers caspase-3, Bax, and Bcl-2 were measured, and OUA-treated rats showed greater levels of caspase-3, Bax, and lower levels of Bcl-2. On the other hand, reduction in mitochondrial ETC complex enzymes has been associated with a significant increase in inflammatory cytokines $\text{TNF-}\alpha$ and $\text{IL-1}\beta$. Furthermore, this study looked into the effect of OUA on Na^+/K^+ ATPase activity, which was found to be decreased after the OUA injection. Our investigation demonstrated that when rats were repeatedly exposed to OUA, the amounts of neurotransmitters changed. Neurotransmitters have a variety of diverse effects on the brain. Several neurons in the brain release acetylcholine, which has been connected to memory and learning [85,86], circadian rhythms [87],

antinociception [88,89], locomotion [90,91], and the sleep-wake cycle [92,93]. Serotonin is a neurotransmitter that has several effects in the brain that are regulated by various serotonergic receptors [94], involved in cognition [95], learning, memory, and attention [96,97], emotions [98], stress, mood [99,100], movement [101], and sleep [102]. Glutamate, a primary excitatory neurotransmitter in the brain, is also implicated in long-term potentiation and long-term depression (synaptic plasticity). These two processes are associated with memory and learning [103] and neurogenesis [104]. Dopamine is a monoamine neurotransmitter that is involved in a variety of brain functions, including motor function control and learning new motor skills [105,106], pleasure and reward-seeking behavior [107,108], addiction [109], cognition [110,111], pain process [112,113], gastrointestinal motility [114,115]. Neurotoxic effects of OUA in rats are shown by decreased serotonin and acetylcholine levels and increased dopamine and glutamate levels. Oxidative stress is a major cause of neurodegenerative disorders. Treatment with OUA raises MDA, Nitrite, AChE, and LDH levels while decreasing antioxidant enzymes SOD and GSH levels.

Our findings revealed that twenty days of chronic treatment with SNL40, 80 mg/kg in ICV injection to OUA-treated rats resulted in a significant improvement in body weight. In addition, there was a reduction in locomotor activity measured by the actophotometer. The high dose-response of SNL shows a significant improvement in behavioural abnormalities. In contrast, the standard drug lithium alone and in combination with SNL high dose exhibited a significant improvement in behavioural alterations compared to SNL alone treated rats.

Current research indicates that SIRT-1 levels in CSF, brain homogenate, and blood plasma samples increase after continuous SNL40 and SNL80 mg/kg treatment. Furthermore, Li-treated groups restored SIRT-1 protein levels more efficiently than SNL-treated groups in rat brain homogenate, blood plasma, and CSF samples. On the other hand, the apoptotic marker level in blood plasma and brain homogenate shows a decrease in caspase-3 and Bax and an increase in Bcl-2. Furthermore, the results show that continuous SNL treatment recovers mitochondrial ETC-complexes enzyme levels Complex I, II, IV, and V, as well as CoQ10 in brain homogenate. SNL administration reduces neuronal inflammation, as evidenced by lower levels of TNF- α and IL-1 β in blood plasma and rat brain homogenate. Furthermore, SNL increased serotonin and acetylcholine levels while lowering dopamine and glutamate levels in rat brain homogenates.

Oxidative damage in OUA-treated rats with SNL40 and 80 mg/kg, on the other hand, shows a reduction in oxidative stress as seen by a significant decrease in MDA, Nitrite AChE, and LDH levels. In addition, there was a significant rise in the amount of anti-oxidant markers SOD and GSH in brain homogenate. Additionally, after continuous treatment with SNL40 and SNL80 mg/kg, Na⁺/K⁺ ATPase enzyme activity increased in rat brain homogenate, although Li-treated groups restored activity more effectively than SNL-treated groups. The Li60 mg/kg alone and Li60 mg/kg in conjunction with SNL80 mg/kg treated groups restored the altered Na⁺/K⁺ ATPase enzyme levels more successfully than the SNL80 mg/kg SNL40 mg/kg treated groups in brain homogenate samples.

As a result, the current study indicates that ICV-OUA administration reduces SIRT-1 protein levels and neuronal death in rats. Furthermore, there was a reduction of mitochondrial ETC complexes in the disease condition and an increase in inflammation and oxidative stress. Prolonged SNL and Li therapy produces improvements and significant dose-dependent restorations. As a result, these SIRT-1 and SNL activators exerted neuroprotective effects following OUA-mediated BD rat model ICV injections.

Although the current findings are just correlations, they suggest SNL reduced SIRT-1 protein levels in rats with BD-like behavioural and neurochemical symptoms in OUA-induced BD. Our findings suggest that SIRT-1 levels in brain tissue, blood plasma, and CSF can be used as an effective and reliable early diagnostic biomarker for predicting neurological dysfunctions. Lithium works as a mood stabilizer drug to counteract these pathological changes that assist in alleviating BD symptoms. Our studies show that SNL's

neuroprotective potential allows for developing a new disease-modifying treatment for the neurodegenerative disease by SIRT-1 signalling activation in the brain.

Ouabain is a powerful inhibitor of the sodium potassium ATPase pump, which is situated on the cell's outer plasma membrane. Manic episodes are marked by ion dysregulation, which is a common and long-lasting symptom. Acute maniacs have been found to have heightened levels of calcium and sodium in their cells, as well as increased lithium retention and impaired sodium pump activity. People with bipolar disorder may also have a reduced expression of the alpha2 subunit of the sodium pump in their brains, as well as lower levels of endogenous cardiolipids in their blood. The pathophysiology of manic and depressive episodes appears to be mediated by a decrease in the activity of the brain's sodium and potassium-activated adenosine triphosphatase (Na, K-ATPase). It's possible that such a change affects neuronal activity and excitability directly, activating a second message in the absence of a first (neurotransmitter). Thus, persistent use of Ouabain alters neuronal signalling and alters neurotransmitter levels at the synapse, resulting in behavioural changes.

In this investigation, we found that Ouabain treatment reduced serotonin and acetylcholine concentrations significantly. Serotonin deficiency causes anxiety and depression, as well as changes in motor activity. Acetylcholine deficiency has been linked to memory loss and confusion. All of these alterations are in line with the signs and symptoms of someone who is suffering from bipolar disorder. For this reason, we performed several different tests to assess the anxiety and depressive-like behaviour, as well as locomotor activity to test the hyperlocomotion induced by ouabain administration. Therefore, in order to evaluate these changes we have performed several different parameters such as open field test and force swim test to measure the anxiety and depressive like behaviour, locomotor activity to test the hyperlocomotion induced by the ouabain administration. As food intake is a primary indicator of anxiety and depression, body weight was also evaluated as part of the study. Ouabain administration has also been shown to increase the apoptotic signalling pathway, activate NLRP3 inflammasomes, and produce inflammation, as well as generate oxidative and nitrosative stress.

Consequently, in order to examine the effects of ouabain on the cellular and molecular levels, we have carried out a variety of neurochemical analyses, such as evaluating the levels of antioxidant enzymes to examine the oxidative stress induced etc. Neurochemical study of ouabain's effect on the brain included testing for the levels of TNF- α and IL-1- β , as well as markers of apoptosis such as caspase-3, Bax, and Bcl-2, to gain a better sense of the magnitude of inflammation caused by ouabain. Also, histology and neurotransmitter levels were measured to acquire a better sense of the effects of ouabain administration. All these characteristics put together allowed us to reach the conclusion that our medicine solanesol has the potential to be a useful treatment in the future.

Limitations: The proposed OUA model could explore disease aetiology and screen potential mood stabilizer drug candidates. A mechanistic approach must be validated using sirtuin gene knock-in or knock-out experiments. A correlative study, such as Western Blot for cellular markers, is also necessary to offer molecular support for this hypothesis.

4. Material and Methods

4.1. Experimental Animals

Adult Wistar rats (220–250 gm, nine weeks of age, either sex) were collected from the ISF College of Pharmacy, Central Animal House in Moga, Punjab. These animals were evenly divided and housed in polyacrylic cages with a wiremesh top and soft bedding under typical husbandry circumstances of a 12-h reverse light cycle, free access to food and water, and a temperature of 23 ± 2 °C. According to the requirements of the Government of India, the experimental procedure was approved by the Institutional Animal Ethics Committee (IAEC) with a registration number. 816/PO/ReBiBt/S/04/CPCSEA as protocol no. ISFCP/IAEC/CPCSEA/Meeting No: 28/2020/Protocol No. 463. Animals were acclimatized to laboratory conditions before being used in experiments.

4.2. Drugs and Chemicals

OUA was purchased from Sigma–Aldrich (St. Louis, MO, USA). Ex-gratia samples of SNL from BAPEX, New Delhi (India) and Lithium carbonate from Sun Pharma, Mumbai, India were provided. All of the other chemicals employed in the experiment were of analytical grade. Before use, the medication and chemical solutions were freshly made. Oral administration of SNL dissolved in water (with 2% ethanol) (p.o.) [116].

4.3. Experimental Animal Grouping

A total of 48 Wistar rats (either sex), nine weeks old, were employed during the 28-day protocol schedule. These rats were kept in a polyacrylic cage with a wire mesh top and soft bedding (38 cm 32 cm 16 cm; 3–4 rats per cage) at a regulated temperature (22 ± 2 °C) and humidity (65–70%) with artificial illumination (12 h/12 h light/dark cycle, lights on at 6:00 a.m.). Their bedding consisted of residue-free wood shavings that had been sanitized. The male rats were housed separately from the female rats to run the whole experiment smoothly because the experiment lasted for a whole month. If the rats of both sexes were housed together, it might result in pregnancy or other complications that would invalidate the study's findings. These animals had unrestricted access to a standard chow diet and purified water. To avoid the effects of the circadian rhythm, the entire experimental protocol schedule was completed between 9:00 AM and 1:00 PM. They were randomly divided into eight groups ($n = 6$ per group). Group 1 vehicle control; Group 2 Sham control; Group 3 SNL *per se* (80 mg/kg p.o.); Group 4 OUA (1 mM/0.5 μ L/5 min/Unilateral/ICV injection); Group 5 OUA + SNL (40 mg/kg, p.o.); Group 6 OUA + SNL (80 mg/kg p.o.); Group 7 OUA + Li (60 mg/kg, i.p.), and Group 8 OUA + Li + SNL80. Several behavioral parameters were measured from the first to the 28th day (Forced swim test, Open field test, and Locomotor activity). The 28th day was marked by collecting biological samples (CSF and blood plasma) from Wistar adult rats. The animals were fully anesthetized with sodium pentobarbital (270 mg/mL, i.p.), and then fresh brains were preserved in ice-cold PBS (0.1 M) of PBS for further biochemical evaluation. The biochemical estimation of SIRT-1 protein level determination in brain homogenate, blood plasma, and CSF was performed on the 29th and 30th days. Oxidative indicators (MDA, GSH, SOD, Nitrite, AChE, LDH) were also measured in brain homogenates. Similarly, apoptotic markers (Caspase-3, Bax, Bcl-2) and mitochondrial ETC-complexes enzymes (Complex-I, II, IV, V, and CoQ10) in the brain homogenate and blood plasma were also examined. Inflammatory markers (IL-1, TNF- α) and neurotransmitters (Ach, Dopamine, 5-HT, Glutamate) were also measured in brain homogenate and blood plasma. The protocol for the experiment is summarized in (Figure 13).

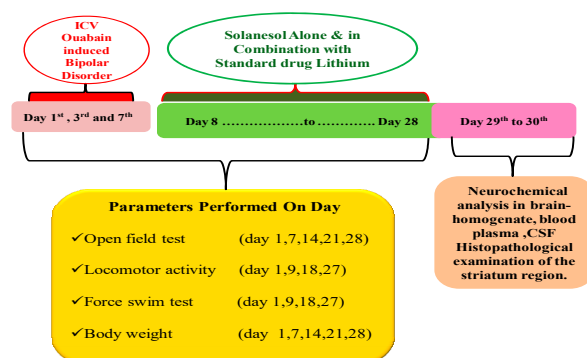


Figure 13. Experimental protocol schedule (Behavioral & Neurochemical estimations).

4.4. ICV-OUA Induced Experimental Animal Model of BD

Mehan and colleagues effectively validated, established, and improved the OUA-induced BD experimental model in adult rats, in which ICV infusion of OUA on alternate days in rats brain develops bipolar disorder-like alterations by performing several be-

havioural parameters. Three days of OUA-ICV injection (1 mM/0.5 µL) were given to the rats in the experiment. According to Valvassori et al., OUA generates neurological damage similar to that shown in an experimental animal model of BD. It is a valid model for examining pathophysiological alterations similar to those seen in BD [117].

The rats were habituated to the laboratory environment. After acclimatization, all animals in the experimental groups were anaesthetized with ketamine (75 mg/kg, i.p.) before being placed in a stereotaxic frame [40]. The skull was exposed after shaving the head and cutting a midline scalp incision. With the tooth bar set at 0 mm, each animal's skin overlying the skull and the striatum coordinates must be precisely measured (AP-1.0 mm; ML-2.5 mm; DV-3.5 mm) [117]. Then, according to the protocol schedule, all animals in the experimental groups received OUA (1 mM/0.5 µL/5 min/Unilateral/ICV injection) for three days (1st, 3rd, and 7th days). The infusion was administered manually, using a Hamilton syringe, through the burr holes drilled onto the skull surface. The injection rate in the experimental groups was 0.5 µL/5 min, with the needle remaining in place for a further 1 min before being progressively removed. The cannula is sealed with a detachable plastic ear pin. The hole was filled with dental cement before being sutured with an absorbable surgical suture connected to a sterile surgical needle.

Rats were housed individually in a polyacrylic cage that usually contained a warm cloth for post-operative care. Special attention was given to them until they regained spontaneous movement, which generally occurred 2–3 h after anaesthesia. The temperature in the room was kept at 25 ± 3 °C. Milk and glucose water were kept in the cages for 2–3 days to avoid physical trauma after surgery. Gentamycin (35 mg/kg) was given intraperitoneally to rats for three days to prevent sepsis, and lignocaine gel was applied to the sutured area to relieve pain. Neosporin powder was dusted on them to prevent bacterial infection of the skin. After surgery, the body's general health and clinical symptoms such as dehydration were closely examined. After seven days, rats continued to eat healthy food and drink plenty of water, and their spontaneous mobility returned, indicating that they had healed. The protocol drug SNL at 40 and 80 mg and the standard drug Lithium alone and Lithium in combination with SNL80 mg/kg were administered chronically beginning on day 8th and continuing until day 28th. Behavioural parameters such as locomotor activity, open field test, and Forced Swimming Test were carried out following the protocol schedule. After completing the protocol schedule, all animals were decapitated on days 29th and 30th, and their brains were removed to perform biochemical, inflammatory, and neurochemical assessments [118].

4.5. Parameters Assessed

Measurement of Body Weight

According to the protocol schedule, body weight was measured on the experiment's 1st, 7th, 14th, 21st, and 28th days [117].

4.6. Assessment of Behavioural Parameters

4.6.1. Open Field Test (OFT)

The animals exhibited manic-like behavior after a single injection of OUA for three days (1st, 3rd, and 7th). The rat was placed in a cage on the first day and trained to explore an open field for 5 min. During the test, a camera monitored each rat's activities, including an increase in the number of crossings, rearings, and time spent in the centre. According to the protocol schedule, on days 1st, 7th, 14th, 21st, and 28th, an open field test was used to measure the number of crossings, rearings, and time spent in the centre in rats [119].

4.6.2. Locomotor Activity

Increased locomotor activity is a sign of manic-like behaviour [120]. The device uses photocells to detect motor activity. The animals were placed in the activity room for 3 min before the recording for habituation. On the 1st, 9th, 18th, and 27th days after ICV administrations, locomotion was assessed using an actophotometer (INCO {Instruments

and Chemicals Private Limited}, Ambal, Haryana, India) for 5 min, and values were represented as counts per 5 min [121].

4.6.3. Forced Swimming Test (FST)

A Forced Swimming Test was used to evaluate the immobility time. Individual rats were placed in cylindrical tanks (height 50 cm; diameter 15 cm) with 30 cm of water at a temperature of 24 ± 1 °C. A camera filmed the rat's movements for 5 min. During the training session, rats are exposed to the tank for 15 min on the first day and 5 min on the second day. The testing period for rats consists of a single 6-min exposure, with the first 2 min as a habituation period. Each animal was tested for depressive-like behaviour on days 1st, 9th, 18th, and 27th following ICV injection. The immobility time was recorded for 5 min during each session. When the rat stopped struggling and stayed motionless in an upright position in the water, only making slight movements to keep its head above the water, it was determined to be immobile [122].

4.7. Neurochemical Alterations Evaluation

4.7.1. Collection and Preparation of Biological Samples

On day 29th of the experiment, 2.5 mL of blood was collected from anaesthetized rats through retro-bulbar puncture from the orbital venous plexus by inserting a capillary tube medially into the rat eye. Blood from the plexus was collected into a sterile Eppendorf tube via the capillary action through gentle rotation and retraction of the tube [123]. The blood samples were centrifuged at $10,000 \times g$ for 15 min to separate the plasma, and the supernatant was carefully stored in a deep freeze (at -80 °C) for further use.

Following blood collection, rats were deeply anaesthetized with sodium pentobarbital (270 mg/mL, i.p.) and subjected to caudal incision, translucent duramater was exposed, and a 30 gauge needle was gently placed at a 30° angle into the cisterna magna [124]. Approximately 100 μ L CSF was carefully ejected into a 0.5 mL sterile Eppendorf tube using the suction pressure of a 1 mL tuberculin syringe attached to a needle. The collected sample was frozen at -80 °C until analysed ELISA [125].

Immediately after CSF collection, rats were sacrificed by decapitation; whole brains were isolated from the skull with the utmost care, freshly weighed and washed with ice-cold, isotonic saline solution, and then homogenized with 0.1 M (*w/v*) of chilled PBS (pH = 7.4). The rat brain homogenate was centrifuged at $10,000 \times g$ for 15 min, the supernatant was separated, and the aliquots were preserved. The samples were deep-frozen at -80 °C to be used as and when required for various biochemical estimations.

4.7.2. Assessment of Cellular and Molecular Markers

Measurement of SIRT-1 Protein Level

The level of SIRT-1 protein expression was measured using standard ELISA kits (E-EL-R1102/SIRT-1 Elabsciences, Wuhan, China). This test was carried out in the brain homogenate [119], blood plasma [125], and CSF [126] according to the standard technique. The values are given in brain homogenate as nM/ μ g protein [127] and as ng/mL protein in blood plasma [128] and CSF [129].

4.7.3. Assessment of Apoptotic Markers

Measurement of Caspase-3 Level

Caspase-3 concentrations were determined using commercial ELISA kits (E-EL-R0160/Caspase-3 Elabsciences, Wuhan, China). ELISA kits were used to perform this test in brain homogenate [121] and blood plasma [47].

Measurement of Bax and Bcl-2 Levels

Commercial ELISA kits were used to determine the protein levels of Bax and Bcl-2 (E-EL-R0098/Bax/Bcl2 Elabsciences, Wuhan, China). The level of Bax protein in brain homogenate [130] and blood plasma was measured [131]. Using ELISA commercial kits, the

quantities of anti-apoptotic proteins such as Bcl-2 were evaluated in brain homogenate [37] and blood plasma [131].

4.7.4. Assessment of Mitochondrial ETC-Complexes Enzyme Levels

Preparation of Post Mitochondrial Supernatant (PMS) from Rat Whole-Brain Homogenate

The rat whole brain homogenate was centrifuged for 20 min at $5000 \times g$ rpm at 4°C , and the resulting supernatant was used as rat brain PMS for further research. Differential centrifugation was used to prepare the crude mitochondrial fraction. By gently shaking at 4°C for 60 min, the pellet generated during the preparation of PMS was combined with 0.1 M sodium phosphate buffer (pH 7.4) in a 1:10 proportion. The pellets were re-suspended in the same buffer containing extra sucrose at a concentration of 250 mmol/L after centrifugation at $16,000 \times g$ rpm at 0°C for 30 min. The centrifugation and resuspension steps were done three times, and the crude mitochondrial fraction produced in the buffered sucrose solution was used for further investigation [40,132].

Mitochondrial ETC Complex-I Enzyme Activity (NADPH Dehydrogenase)

To determine complex-I activity, the rate of NADH oxidation at 340 nm in an assay medium was measured spectrophotometrically at 37°C for 3 min. Reactions were carried out in the absence and presence of 2 μM rotenone, and the rotenone-sensitive activity was assigned to complex-I [40,133].

Mitochondrial ETC Complex-II Enzyme Activity (Succinate dehydrogenase/SDH)

At 490 nm (Shimadzu, Kyoto, Japan, UV-1700), the absorbance of a 0.3 mL sodium succinate solution in a 50 μL gradient fraction of homogenate was measured. The molar extinction coefficient of the chromophore ($1.36 \times 10^4 \text{ M}^{-1} \text{ cm}^{-1}$) was used to determine the results, which were reported as INT decreased $\mu\text{mol}/\text{mg}$ protein [40,134].

Mitochondrial ETC Complex-IV Enzyme Activity (Cytochrome Oxidase)

Reduced cytochrome-C (0.3 mM) was added to the assay mixture in a 75 mM phosphate buffer. The process was started by adding a solubilized mitochondrial sample, and the absorbance change was measured for 2 min at 550 nm [40].

Mitochondrial ETC Complex-V Enzyme Activity (ATP Synthase)

To inactivate the ATPases, aliquots of homogenates were sonicated immediately in ice-cold perchloric acid (0.1 N). Supernatants containing ATP were neutralized with 1 N NaOH and kept at -80°C until analysis after centrifugation ($14,000 \times g$, 4°C , and 5 min). A reverse-phase HPLC was used to measure the amount of ATP in the supernatants (PerkinElmer). The reference solution of ATP was made according to the dissolving standard, and the detecting wavelength was 254 nm [40,135].

4.7.5. Assessment of Neurotransmitters Levels

Measurement of Brain Serotonin Levels

The level of serotonin in brain homogenate was estimated using the method of Sharma et al. with minor modifications. HPLC with an electrochemical detector and a C18 reverse-phase column was used to determine it. Sodium citrate buffer (pH 4.5)—acetonitrile (87:13, *v/v*) is used in the mobile phase. Ten mmol/L citric acids, 25 mmol/L NaH_2PO_4 , 25 mmol/L EDTA, and two mmol/L 1-heptane sulfonic acid made up the sodium citrate buffer. The electrochemical parameters in the experiments were +0.75 V, with sensitivity ranging from 5 to 50 nA. The separation procedure was performed at a flow rate of 0.8 mL/min. 20 μL of samples were manually injected. On the day of the experiment, brain samples were homogenized in 0.2 mol/L perchloric acids. The samples were then centrifuged for 5 min at $12,000 \times g$ rpm. The supernatant was filtered via 0.22 mm nylon filters before being injected into the HPLC sample injector. With the help of the breeze

program, data were collected and evaluated. Serotonin concentrations were determined from the standard curve using a standard with a 10–100 mg/mL concentration [40].

Assessment of Brain Dopamine Levels

Dopamine levels in striatal tissue samples were measured using Tiwari and colleagues' technique. Dopamine activity in rat brain homogenate is quantified as ng/mg protein [130].

Assessment of Brain Glutamate Levels

According to Alam et al., glutamate was measured in tissue samples after derivatization with *o*-phthalaldehyde/ β -mercaptoethanol (OPA/ β -ME) and quantitative analysis in rat brain homogenates, glutamate activity is reported as ng/mg protein [39].

Assessment of Brain Acetylcholine Levels

A diagnostic kit is used to measure acetylcholine (E-EL-0081/acetylcholine; Elab-sciences, Wuhan, China). All reagents and rat brain homogenate were produced according to the kit's normal procedure. In the microtiter plate, the optical density of the reaction mixture was determined at 540 nm [133].

4.7.6. Assessment of Neuroinflammatory Cytokines

Measurement of TNF- α and IL-1 β Levels

Using a rat ELISA immunoassay kit (E-EL-R0019/TNF- α ; E-EL-R0012/IL-1 β ; ELab-Sciences, Wuhan, China), the level of TNF- α was measured in rat brain homogenate [42] and blood plasma. The activity of IL-1 β was measured in rat brain homogenate and blood plasma as pg./mg protein [130].

4.7.7. Estimation of Oxidative Stress Markers

Measurement of Reduced Glutathione Levels

In the brain homogenate, the level of reduced glutathione was determined. 1 mL supernatant was precipitated with 1 mL 4% sulfosalicylic acid and cold digested for 1 h at 4 °C. The samples were centrifuged for 15 min at 1200 \times g rpm. To 1 mL supernatant, 2.7 mL phosphate buffer (0.1 M, pH 8) and 0.2 mL 5,5'-dithiobis-(2-nitrobenzoic acid) (DTNB) were added. A spectrophotometer was used to measure the yellow color that emerged at 412 nm right away. Glutathione content in the supernatant is given as μ M/mg protein [136].

Measurement of Nitrite Levels

A colourimetric assay utilizing Greiss reagent (0.1% *N*-(1-naphthyl) ethylenediamine dihydrochloride, % sulfanilamide, and % phosphoric acid) determines the concentration of nitrite in the supernatant, which is indicative of the formation of nitric oxide (NO). Equal amounts of supernatant and Greiss reagent are mixed, the mixture is incubated at room temperature in the dark for 10 min, and the absorbance is measured spectrophotometrically at 540 nm. A sodium nitrite standard curve is used to calculate nitrite concentration in the supernatant, which is given as μ M/mg protein [136].

Measurement of Malondialdehyde (MDA) Levels

The MDA end product of lipid peroxidation was determined quantitatively in brain homogenates. A spectrophotometer measured the quantity of MDA after its reaction with thiobarbituric acid at 532 nm. MDA concentration is expressed in nM/mg of protein [137].

Measurement of Superoxide Dismutase (SOD) Levels

SOD activity was evaluated by auto-oxidation of epinephrine at pH 10.4 using spectrophotometry. The brain homogenate supernatant (0.2 mL) was combined with 0.8 mL of 50 mM glycine buffer, pH 10.4, and the reaction was begun with 0.02 mL epinephrine. The absorbance was spectrophotometrically measured at 480 nm after 5 min. The activity of SOD was measured in nM/mg of protein [37].

Measurement of Acetylcholinesterase (AChE) Levels

The levels of acetylcholinesterase (AChE) were measured using spectrophotometry. The 0.05 mL supernatant, 3 mL 0.01 M sodium phosphate buffer (pH 8), 0.10 mL acetylthiocholine iodide, and 0.10 mL DTNB were used in the test mixture (Ellman reagent). The absorbance change was spectrophotometrically recorded at 412 nm right away. In the supernatant, the enzymatic activity is represented as $\mu\text{M}/\text{mg}$ protein [40].

Measurement of Lactate Dehydrogenase (LDH) Assay

A diagnostic kit (Coral Diagnostics, Goa, India) was used to quantify the amount of LDH in the rat brain homogenate, and the amount of LDH was quantified as Units/L [138].

4.7.8. Evaluation of Na^+/K^+ ATPase Activity in Rat Brain Homogenate

The activity of the Na^+/K^+ ATPase enzyme was measured using a spectrophotometer and a calorimetric method-based assay kit (E-BC-K539-M; Na^+/K^+ ATPase ELabSciences, Wuhan, China). The Na^+/K^+ ATPase assay reaction mixture contains 5.0 mM MgCl_2 , 80.0 mM NaCl, 20.0 mM KCl, and 40.0 mM Tris-HCl in a final volume of 200 L with a pH of 7.4. The reaction was begun after a 10-min pre-incubation interval at 37 °C by adding 3.0 mM ATP and incubated for 20 min. Controls were carried out under identical conditions as before, but with the addition of 1.0 mM ouabain. The difference between the two assays was utilized to calculate Na^+/K^+ ATPase activity. The specific activity of the enzyme was measured in nmol of P_i released per minute per mg of protein [139].

4.7.9. Histopathological Examination

After the completion of the protocol schedule, rats were decapitated and their brains removed. The histological appearance of the brain was checked with the hematoxylin and eosin staining method. A specific brain part, i.e., the striatum region, was carefully identified and preserved in 4% paraformaldehyde for further observation. After dehydration, parafinization of the tissue was done, and then the tissue was cut into pieces of the thickness of 5 μm . The tissue was then stained using hematoxylin and eosin dyes, mounted on the glass slide, and covered with the coverslip. The tissue was then observed under a fluorescence microscope for detailed analysis [125].

4.7.10. Protein Estimation

A Coral protein estimation kit (Biuret method) was used to determine the protein content.

4.8. Statistical Analysis

The mean and standard error were used to express all of the findings (SEM). The data were analyzed using a two-way ANOVA followed by a Bonferroni post hoc test and a one-way ANOVA followed by a Tukey's multi-comparison test. It was determined that $p < 0.001$ was statistically significant. The sample size was estimated after the data was confirmed to be normalized, and the normality distribution was checked using the Kolmogorov Smirnov test. GraphPad Prism version 5.03 for Windows generated all statistical results (GraphPad Software, San Diego, CA, USA). The mean and standard error of the mean was used to express the statistical data (SEM).

5. Conclusions

Finally, the research confirms that SNL protects rats from developing BD caused by OUA. This is the first study to link SNL's antioxidant, anti-inflammatory, and anti-apoptotic properties to its potential neuroprotective benefit as a therapy for the management of BD. The amounts of several neurochemicals in brain homogenate, blood plasma, and CSF were examined, revealing that SNL had a central and peripheral protective impact by reducing BD-like alterations. According to the findings, this study can be used as strong evidence that SIRT-1 downregulation and serotonin evaluation can be employed as potential biomarkers for the early detection of BD. The primary limitation of this study is the lack of gross

pathology and immunohistology research on the area-specific molecular mechanistic effect of SNL. As a result, more preclinical research on the knock-in and knock-out of the SIRT-1 gene is required to understand the molecular mechanism better.

Author Contributions: Investigation, original draft, writing review, B.R., P.S., A.P., M.S., S.K. and S.B.; formal analysis, data curation, validation, editing, A.A., M.A., N.A., S.A. and R.K.; conceptualization, resources, supervision, S.M. and A.S.N. All data were generated in-house, and no paper mill was used. All authors agree to be accountable for all aspects of this work, ensuring integrity and accuracy. All authors have read and agreed to the published version of the manuscript.

Funding: This work was supported and funded by institutional grants from the Institutional Animal Ethics Committee (IAEC) with registration No. 816/PO/ReBiBt/S/04/CPCSEA as protocol no. IS-FCP/IAEC/ CPCSEA/Meeting No. 8/2020/Protocol No. 463 approved by RAB Committee, ISFCP, Moga, Punjab, India. The authors are also thankful to the Researchers Supporting Project number (RSP2022R491), King Saud University, Riyadh, Saudi Arabia.

Institutional Review Board Statement: The study was conducted according to the guidelines of the Institutional Animal Ethics Committee (IAEC) with registration No. 816/PO/ReBiBt/S/04/CPCSEA as protocol no. ISFCP/IAEC/CPCSEA/Meeting No. 28/2020/Protocol No. 463 approved by RAB Committee, ISFCP, Moga, Punjab, India.

Informed Consent Statement: Not applicable.

Data Availability Statement: All data generated or analysed during this study are included in this article. There are no separate or additional files.

Acknowledgments: The authors express their gratitude to Chairman Parveen Garg and Director-cum-Principal, G.D. Gupta, ISF College of Pharmacy (An Autonomous College), Moga (Punjab), India, for their incredible vision and support. The authors are also thankful to the Researchers Supporting Project number (RSP2022R491), King Saud University, Riyadh, Saudi Arabia.

Conflicts of Interest: The authors declare no conflict of interest.

Abbreviations

Ach	Acetylcholine
AchE	Acetylcholinesterase
AD	Alzheimer disease
ALS	Amyotrophic lateral sclerosis
ALS	Amyotrophic lateral sclerosis
ANOVA	Analysis of variance
AP-1	Activator protein-1
ATP	Adenosine triphosphate
BAPEX	Bangladesh Petroleum Exploration and Production
BAX	Bcl-2-associated X protein
BD	Bipolar Disorder
BDNF	Brain-derived neurotrophic factor
Ca ²⁺	Calcium
CoQ10	Coenzyme Q10
CSF	Cerebrospinal fluid
CVS	Chronic variable stress
ELISA	Enzyme-linked immunoassay
ERK1/2	Extracellular signaling-regulated protein kinases 1 & 2
ETC	Electron transport chain
FOXO1/3	Fork head box protein O1/3
FST	Forced Swim test
FST	Forced Swimming Test
GSH	Glutathione
HD	Huntington disease
HPLC	High performance liquid chromatography
5-HT	Serotonin

IAEC	Institutional Animal Ethics Committee
ICH	Intracerebral haemorrhage
ICV	Intracerebroventricular
IL-1 β	Interleukin-1 β
IP	Intraperitoneal
LDH	Lactate dehydrogenase
LDH	lactate dehydrogenase
Li	Lithium
MDA	Malondialdehyde
MDA	malondialdehyde
MS	Multiple sclerosis
Na ⁺ K ⁺ -ATPase	Sodium and potassium-activated adenosine triphosphatase
NAD ⁺	Nicotinamide adenine dinucleotide
NADH	Nicotinamide adenine dinucleotide hydrogen
NF- κ B	Nuclear factor kappa light chain enhancer of activated B-cells
OFT	Open field test
OPA/ β -ME	O-phthalaldehyde/ β -mercaptoethanol
OUA	Ouabain
p53	Tumour proteins p53
PD	Parkinson's disease
PGC-1	Peroxisome proliferator-activated gamma co-activator-1
PO	Per oral
RNS	Reactive nitrogen species
ROS	Reactive oxygen species
SDH	Succinate dehydrogenase
SEM	Standard error of the mean
SIRT-1	Silent mating-type information regulation 2 homolog-1
SNL	solanesol
SOD	superoxide dismutase
TNF- α	Tumour necrosis factor-alpha
v/v	volume/volume

References

- Jia, X.; Goes, F.S.; Locke, A.E.; Palmer, D.; Wang, W.; Cohen-Woods, S.; Genovese, G.; Jackson, A.U.; Jiang, C.; Kvale, M.; et al. Investigating rare pathogenic/likely pathogenic exonic variation in bipolar disorder. *Mol. Psychiatry* **2021**, *26*, 5239–5250. [CrossRef]
- Jain, A.; Mitra, P. Bipolar Affective Disorder. In *StatPearls*; StatPearls Publishing: Treasure Island, FL, USA, 2022; pp. 1–25. Available online: <https://www.ncbi.nlm.nih.gov/books/NBK558998/> (accessed on 1 May 2022).
- Dong, M.; Lu, L.; Zhang, L.; Zhang, Q.; Ungvari, G.S.; Ng, C.; Yuan, Z.; Xiang, Y.; Wang, G.; Xiang, Y.-T. Prevalence of suicide attempts in bipolar disorder: A systematic review and meta-analysis of observational studies. *Epidemiol. Psychiatr. Sci.* **2020**, *29*, 1–9. [CrossRef] [PubMed]
- Uher, R.; Zwickler, A. Etiology in psychiatry: Embracing the reality of poly-gene-environmental causation of mental illness. *World Psychiatry* **2017**, *16*, 121–129. [CrossRef]
- Serra, G.; Koukopoulos, A.; De Chiara, L.; Sani, G.; Tondo, L.; Girardi, P.; Reginaldi, D.; Baldessarini, R. Early clinical predictors and correlates of long-term morbidity in bipolar disorder. *Eur. Psychiatry* **2017**, *43*, 35–43. [CrossRef]
- Mullins, N.; Forstner, A.J.; O'Connell, K.S.; Coombes, B.; Coleman, J.R.; Qiao, Z.; Als, T.D.; Bigdeli, T.B.; Børte, S.; Bryois, J.; et al. Genome-wide association study of more than 40,000 bipolar disorder cases provides new insights into the underlying biology. *Nat. Genet.* **2021**, *53*, 817–829. [CrossRef]
- Hirschfeld, R. Differential diagnosis of bipolar disorder and major depressive disorder. *J. Affect. Disord.* **2014**, *169*, S12–S16. [CrossRef]
- Jornada, L.K.; Valvassori, S.S.; Steckert, A.V.; Moretti, M.; Mina, F.; Ferreira, C.L.; Arent, C.O.; Pizzol, F.D.; de Quevedo, J.L. Lithium and valproate modulate antioxidant enzymes and prevent ouabain-induced oxidative damage in an animal model of mania. *J. Psychiatr. Res.* **2011**, *45*, 162–168. [CrossRef]
- Valvassori, S.S.; Resende, W.R.; Lopes-Borges, J.; Mariot, E.; Dal-Pont, G.C.; Vitto, M.F.; Luz, G.; de Souza, C.T.; Quevedo, J. Effects of mood stabilizers on oxidative stress-induced cell death signaling pathways in the brains of rats subjected to the ouabain-induced animal model of mania: Mood stabilizers exert protective effects against ouabain-induced activation of the cell death pathway. *J. Psychiatr. Res.* **2015**, *65*, 63–70.

10. Ladol, S.; Sharma, D. Pharmacotherapeutic Effects of Hippophaerhamnoides in Rat Model of Post-traumatic Epilepsy in View of Oxidative Stress, Na⁺, K⁺ ATPase Activity and Sodium Ion Channel Expression. *Acta Sci. Neurol.* **2021**, *4*. Available online: <https://actascientific.com/ASNE/pdf/ASNE-04-0359.pdf> (accessed on 1 May 2022).
11. Krishnan, V.; Nestler, E.J. Animal Models of Depression: Molecular Perspectives. *Mol. Funct. Models Neuropsychiatry* **2011**, *7*, 121–147. [[CrossRef](#)]
12. Valvassori, S.S.; Budni, J.; Varela, R.B.; Quevedo, J. Contributions of animal models to the study of mood disorders. *Rev. Bras. Psiquiatr.* **2013**, *35*, S121–S131. [[CrossRef](#)] [[PubMed](#)]
13. Lopes-Borges, J.; Valvassori, S.S.; Varela, R.B.; Tonin, P.T.; Vieira, J.S.; Gonçalves, C.L.; Streck, E.L.; Quevedo, J. Histone deacetylase inhibitors reverse manic-like behaviors and protect the rat brain from energetic metabolic alterations induced by ouabain. *Pharmacol. Biochem. Behav.* **2015**, *128*, 89–95. [[CrossRef](#)] [[PubMed](#)]
14. Schwartz, M.W.; Woods, S.C.; Porte, D., Jr.; Seeley, R.J.; Baskin, D.G. Central nervous system control of food intake. *Nature* **2000**, *404*, 661–671. [[CrossRef](#)] [[PubMed](#)]
15. Michan, S.; Sinclair, D. Sirtuins in mammals: Insights into their biological function. *Biochem. J.* **2007**, *404*, 1–13. [[CrossRef](#)] [[PubMed](#)]
16. Li, X.-H.; Chen, C.; Tu, Y.; Sun, H.-T.; Zhao, M.-L.; Cheng, S.-X.; Qu, Y.; Zhang, S. Sirt1 Promotes Axonogenesis by Deacetylation of Akt and Inactivation of GSK3. *Mol. Neurobiol.* **2013**, *48*, 490–499. [[CrossRef](#)] [[PubMed](#)]
17. Herskovits, A.Z.; Guarente, L. SIRT1 in Neurodevelopment and Brain Senescence. *Neuron* **2014**, *81*, 471–483. [[CrossRef](#)] [[PubMed](#)]
18. Donmez, G.; Outeiro, T.F. SIRT1 and SIRT2: Emerging targets in neurodegeneration. *EMBO Mol. Med.* **2013**, *5*, 344–352. [[CrossRef](#)] [[PubMed](#)]
19. Aguirre-Rueda, D.; Guerra-Ojeda, S.; Aldasoro, M.; Iradi, A.; Obrador, E.; Ortega, A.; Mauricio, M.D.; Vila, J.M.; Valles, S.L. Astrocytes protect neurons from A β 1-42 peptide-induced neurotoxicity increasing TFAM and PGC-1 and decreasing PPAR- γ and SIRT-1. *Int. J. Med. Sci.* **2015**, *12*, 48. [[CrossRef](#)] [[PubMed](#)]
20. Alcendor, R.R.; Gao, S.; Zhai, P.; Zablocki, D.; Holle, E.; Yu, X.; Tian, B.; Wagner, T.; Vatner, S.F.; Sadoshima, J. Sirt1 Regulates Aging and Resistance to Oxidative Stress in the Heart. *Circ. Res.* **2007**, *100*, 1512–1521. [[CrossRef](#)]
21. Bartoli-Leonard, F.; Wilkinson, F.L.; Schiro, A.; Inglott, F.S.; Alexander, M.Y.; Weston, R. Suppression of SIRT1 in Diabetic Conditions Induces Osteogenic Differentiation of Human Vascular Smooth Muscle Cells via RUNX2 Signalling. *Sci. Rep.* **2019**, *9*, 878. [[CrossRef](#)] [[PubMed](#)]
22. Elibol, B.; Kilic, U. High Levels of SIRT1 Expression as a Protective Mechanism against Disease-Related Conditions. *Front. Endocrinol.* **2018**, *9*, 614. [[CrossRef](#)] [[PubMed](#)]
23. Li, K.; Lv, G.; Pan, L. Sirt1 alleviates LPS induced inflammation of periodontal ligament fibroblasts via downregulation of TLR4. *Int. J. Biol. Macromol.* **2018**, *119*, 249–254. [[CrossRef](#)]
24. Nilni, E.A. The metabolic sensor Sirt1 and the hypothalamus: Interplay between peptide hormones and pro-hormone convertases. *Mol. Cell. Endocrinol.* **2016**, *438*, 77–88. [[CrossRef](#)]
25. Baldo, B.; Gabery, S.; Soyulu-Kucharz, R.; Cheong, R.Y.; Henningsen, J.B.; Englund, E.; McLean, C.; Kirik, D.; Halliday, G.; Petersén, Å. SIRT1 is increased in affected brain regions and hypothalamic metabolic pathways are altered in Huntington disease. *Neuropathol. Appl. Neurobiol.* **2019**, *45*, 361–379. [[CrossRef](#)] [[PubMed](#)]
26. Lee, J.; Kim, Y.; Liu, T.; Hwang, Y.J.; Hyeon, S.J.; Im, H.; Lee, K.; Alvarez, V.E.; McKee, A.C.; Um, S.J.; et al. SIRT3 deregulation is linked to mitochondrial dysfunction in Alzheimer’s disease. *Aging Cell* **2018**, *17*, e12679. [[CrossRef](#)] [[PubMed](#)]
27. Yang, H.; Zhang, W.; Pan, H.; Feldser, H.G.; Lainez, E.; Miller, C.; Leung, S.; Zhong, Z.; Zhao, H.; Sweitzer, S.; et al. SIRT1 activators suppress inflammatory responses through promotion of p65 deacetylation and inhibition of NF- κ B activity. *PLoS ONE* **2021**, e46364. [[CrossRef](#)] [[PubMed](#)]
28. Iside, C.; Scafuro, M.; Nebbioso, A.; Altucci, L. SIRT1 Activation by Natural Phytochemicals: An Overview. *Front. Pharmacol.* **2020**, *11*, 1225. [[CrossRef](#)] [[PubMed](#)]
29. Ma, L.; Dong, W.; Wang, R.; Li, Y.; Xu, B.; Zhang, J.; Zhao, Z.; Wang, Y. Effect of caloric restriction on the SIRT1/mTOR signaling pathways in senile mice. *Brain Res. Bull.* **2015**, *116*, 67–72. [[CrossRef](#)]
30. Feng, Y.; Liu, T.; Dong, S.-Y.; Guo, Y.-J.; Jankovic, J.; Xu, H.; Wu, Y.-C. Rotenone affects p53 transcriptional activity and apoptosis via targeting SIRT1 and H3K9 acetylation in SH-SY5Y cells. *J. Neurochem.* **2015**, *134*, 668–676. [[CrossRef](#)]
31. Singh, P.; Hanson, P.S.; Morris, C.M. SIRT1 ameliorates oxidative stress induced neural cell death and is down-regulated in Parkinson’s disease. *BMC Neurosci.* **2017**, *18*, 1–13. [[CrossRef](#)] [[PubMed](#)]
32. Zhou, C.; Wu, Y.; Ding, X.; Shi, N.; Cai, Y.; Pan, Z.Z. SIRT1 Decreases Emotional Pain Vulnerability with Associated CaMKII α Deacetylation in Central Amygdala. *J. Neurosci.* **2020**, *40*, 2332–2342. [[CrossRef](#)] [[PubMed](#)]
33. Abe-Higuchi, N.; Uchida, S.; Yamagata, H.; Higuchi, F.; Hobara, T.; Hara, K.; Kobayashi, A.; Watanabe, Y. Hippocampal Sirtuin 1 Signaling Mediates Depression-like Behavior. *Biol. Psychiatry* **2016**, *80*, 815–826. [[CrossRef](#)] [[PubMed](#)]
34. Ferland, C.L.; Hawley, W.R.; Puckett, R.E.; Wineberg, K.; Lubin, F.D.; Dohanich, G.P.; Schrader, L.A. Sirtuin Activity in Dentate Gyrus Contributes to Chronic Stress-Induced Behavior and Extracellular Signal-Regulated Protein Kinases 1 and 2 Cascade Changes in the Hippocampus. *Biol. Psychiatry* **2013**, *74*, 927–935. [[CrossRef](#)] [[PubMed](#)]
35. Zhu, L.; Sun, C.; Ren, J.; Wang, G.; Ma, R.; Sun, L.; Yang, D.; Gao, S.; Ning, K.; Wang, Z.; et al. Stress-induced precocious aging in PD-patient iPSC-derived NSCs may underlie the pathophysiology of Parkinson’s disease. *Cell Death Dis.* **2019**, *10*, 1–7. [[CrossRef](#)] [[PubMed](#)]

36. Rajdev, K.; Siddiqui, E.M.; Jadaun, K.S.; Mehan, S. Neuroprotective potential of solanesol in a combined model of intracerebral and intraventricular hemorrhage in rats. *IBRO Rep.* **2020**, *8*, 101–114. [[CrossRef](#)] [[PubMed](#)]
37. Sharma, R.; Rahi, S.; Mehan, S. Neuroprotective potential of solanesol in intracerebroventricular propionic acid induced experimental model of autism: Insights from behavioral and biochemical evidence. *Toxicol. Rep.* **2019**, *6*, 1164–1175. [[CrossRef](#)]
38. Yan, N.; Liu, Y.; Gong, D.; Du, Y.; Zhang, H.; Zhang, Z. Solanesol: A review of its resources, derivatives, bioactivities, medicinal applications, and biosynthesis. *Phytochem. Rev.* **2015**, *14*, 403–417. [[CrossRef](#)]
39. Alam, M.M.; Minj, E.; Yadav, R.K.; Mehan, S. Neuroprotective Potential of Adenyl Cyclase/cAMP/CREB and Mitochondrial CoQ10 Activator in Amyotrophic Lateral Sclerosis Rats. *Curr. Bioact. Compd.* **2020**, *16*, 53–69. [[CrossRef](#)]
40. Sharma, N.; Upadhayay, S.; Shandilya, A.; Sahu, R.; Singh, A.; Rajkhowa, B.; Mehan, S. Neuroprotection by solanesol against ethidium bromide-induced multiple sclerosis-like neurobehavioral, molecular, and neurochemical alterations in experimental rats. *Phytomed. Plus* **2021**, *1*, 100051. [[CrossRef](#)]
41. Sándor, P.S.; Di Clemente, L.; Coppola, G.; Saenger, U.; Fumal, A.; Magis, D.; Seidel, L.; Agosti, R.M.; Schoenen, J. Efficacy of coenzyme Q10 in migraine prophylaxis: A randomized controlled trial. *Neurology* **2005**, *64*, 713–715. [[CrossRef](#)]
42. Upadhayay, S.; Mehan, S.; Prajapati, A.; Sethi, P.; Suri, M.; Zawawi, A.; Almashjary, M.N.; Tabrez, S. Nrf2/HO-1 Signaling Stimulation through Acetyl-11-Keto-Beta-Boswellic Acid (AKBA) Provides Neuroprotection in Ethidium Bromide-Induced Experimental Model of Multiple Sclerosis. *Genes* **2022**, *13*, 1324. [[CrossRef](#)] [[PubMed](#)]
43. Shults, C.W.; Haas, R. Clinical trials of coenzyme Q10 in neurological disorders. *BioFactors* **2005**, *25*, 117–126. [[CrossRef](#)] [[PubMed](#)]
44. Matthews, R.T.; Yang, L.; Browne, S.; Baik, M.; Beal, M.F. Coenzyme Q10 administration increases brain mitochondrial concentrations and exerts neuroprotective effects. *Proc. Natl. Acad. Sci. USA* **1998**, *95*, 8892–8897. [[CrossRef](#)] [[PubMed](#)]
45. DeLegge, M.H.; Smoke, A. Neurodegeneration and inflammation. *Nutr. Clin. Pract.* **2008**, *23*, 35–41. [[CrossRef](#)]
46. Forester, B.P.; Harper, D.G.; Georgakas, J.; Ravichandran, C.; Madurai, N.; Cohen, B.M. Antidepressant Effects of Open Label Treatment with Coenzyme Q10 in Geriatric Bipolar Depression. *J. Clin. Psychopharmacol.* **2015**, *35*, 338. [[CrossRef](#)]
47. Song, J.; Jiao, Y.; Zhang, T.; Zhang, Y.; Huang, X.; Li, H.; Wu, H. Longitudinal Changes in Plasma Caspase-1 and Caspase-3 during the First 2 Years of HIV-1 Infection in CD4Low and CD4High Patient Groups. *PLoS ONE* **2015**, *10*, e0121011. [[CrossRef](#)] [[PubMed](#)]
48. Mahmoud, A.R.; Ali, F.E.; Abd-Elhamid, T.H.; Hassanein, E.H. Coenzyme Q10 protects hepatocytes from ischemia reperfusion-induced apoptosis and oxidative stress via regulation of Bax/Bcl-2/PUMA and Nrf-2/FOXO-3/Sirt-1 signaling pathways. *Tissue Cell* **2019**, *60*, 1–3. [[CrossRef](#)] [[PubMed](#)]
49. Jaswal, P.; Riya, R.; Singh, G. Neuroprotective potential of Solanesol and Epigallocatechin gallate on ICV-STZ induced cognitive dysfunction in rats. *J. Neurol. Sci.* **2019**, *405*, 19. [[CrossRef](#)]
50. Mehan, S.; Monga, V.; Rani, M.; Dudi, R.; Ghimire, K. Neuroprotective effect of solanesol against 3-nitropropionic acid-induced Huntington's disease-like behavioral, biochemical, and cellular alterations: Restoration of coenzyme-Q10-mediated mitochondrial dysfunction. *Indian J. Pharmacol.* **2018**, *50*, 309. [[CrossRef](#)] [[PubMed](#)]
51. El-Mallakh, R.S.; Wyatt, R.J. The Na,K-ATPase hypothesis for bipolar illness. *Biol. Psychiatry* **1995**, *37*, 235–244. [[CrossRef](#)]
52. Banerjee, U.; Dasgupta, A.; Rout, J.K.; Singh, O.P. Effects of lithium therapy on Na⁺-K⁺-ATPase activity and lipid peroxidation in bipolar disorder. *Prog. Neuro-Psychopharmacol. Biol. Psychiatry* **2012**, *37*, 56–61. [[CrossRef](#)] [[PubMed](#)]
53. El-Mallakh, R.S. The Na, K-ATPase hypothesis for manic-depression. I. General considerations. *Med. Hypotheses* **1983**, *12*, 253–268. [[CrossRef](#)]
54. Dudev, T.; Mazmanian, K.; Weng, W.-H.; Grauffel, C.; Lim, C. Free and Bound Therapeutic Lithium in Brain Signaling. *Acc. Chem. Res.* **2019**, *52*, 2960–2970. [[CrossRef](#)] [[PubMed](#)]
55. Pisanu, C.; Heilbronner, U.; Squassina, A. The Role of Pharmacogenomics in Bipolar Disorder: Moving towards Precision Medicine. *Mol. Diagn. Ther.* **2018**, *22*, 409–420. [[CrossRef](#)] [[PubMed](#)]
56. Monti, J.M. The effect of second-generation antipsychotic drugs on sleep parameters in patients with unipolar or bipolar disorder. *Sleep Med.* **2016**, *23*, 89–96. [[CrossRef](#)]
57. Joas, E.; Karanti, A.; Song, J.; Goodwin, G.M.; Lichtenstein, P.; Landén, M. Pharmacological treatment and risk of psychiatric hospital admission in bipolar disorder. *Br. J. Psychiatry* **2017**, *210*, 197–202. [[CrossRef](#)] [[PubMed](#)]
58. McInerney, S.J.; Kennedy, S.H. Review of Evidence for Use of Antidepressants in Bipolar Depression. *Prim. Care Companion CNS Disord.* **2014**, *16*, 23075. [[CrossRef](#)]
59. Ješko, H.; Wencel, P.; Strosznajder, R.; Strosznajder, J. Sirtuins and Their Roles in Brain Aging and Neurodegenerative Disorders. *Neurochem. Res.* **2017**, *42*, 876–890. [[CrossRef](#)]
60. Leite, J.A.; Ghirotto, B.; Targhetta, V.P.; de Lima, J.; Câmara, N.O.S. Sirtuins as pharmacological targets in neurodegenerative and neuropsychiatric disorders. *J. Cereb. Blood Flow Metab.* **2022**, *179*, 1496–1511. [[CrossRef](#)] [[PubMed](#)]
61. Tang, B.L. Sirtuins as modifiers of Parkinson's disease pathology. *J. Neurosci. Res.* **2017**, *95*, 930–942. [[CrossRef](#)]
62. Duan, W. Targeting Sirtuin-1 in Huntington's Disease: Rationale and Current Status. *CNS Drugs* **2013**, *27*, 345–352. [[CrossRef](#)] [[PubMed](#)]
63. Kupis, W.; Pałyga, J.; Tomal, E.; Niewiadomska, E. The role of sirtuins in cellular homeostasis. *J. Physiol. Biochem.* **2016**, *72*, 371–380. [[CrossRef](#)]
64. Shah, S.A.; Khan, M.; Jo, M.H.; Jo, M.G.; Amin, F.U.; Kim, M.O. Melatonin stimulates the SIRT1/Nrf2 signaling pathway counteracting lipopolysaccharide (LPS)-induced oxidative stress to rescue postnatal rat brain. *CNS Neurosci. Ther.* **2017**, *23*, 33–44. [[CrossRef](#)] [[PubMed](#)]

65. Lima, L.F.; Saliba, S.W.; Andrade, J.M.O.; Cunha, M.L.; Cassini-Vieira, P.; Feltenberger, J.D.; Barcelos, L.S.; Guimaraes, A.; De-Paula, A.M.B.; De Oliveira, A.C.P.; et al. Neurodegeneration Alters Metabolic Profile and Sirt 1 Signaling in High-Fat-Induced Obese Mice. *Mol. Neurobiol.* **2017**, *54*, 3465–3475. [[CrossRef](#)] [[PubMed](#)]
66. Fujita, Y.; Yamashita, T. Sirtuins in Neuroendocrine Regulation and Neurological Diseases. *Front. Neurosci.* **2018**, *12*, 778. [[CrossRef](#)] [[PubMed](#)]
67. Logan, R.; McClung, C. Animal models of bipolar mania: The past, present and future. *Neuroscience* **2016**, *321*, 163–188. [[CrossRef](#)]
68. Valvassori, S.S.; Dal-Pont, G.C.; Resende, W.R.; Jornada, L.K.; Peterle, B.R.; Machado, A.G.; Farias, H.R.; de Souza, C.T.; Carvalho, A.F.; Quevedo, J. Lithium and valproate act on the GSK-3 β signaling pathway to reverse manic-like behavior in an animal model of mania induced by ouabain. *Neuropharmacology* **2017**, *117*, 447–459. [[CrossRef](#)]
69. Wang, Y.-C.; Yu, Y.H.; Tsai, M.-L.; Huang, A.C.W. Motor function in an animal model with ouabain-induced bipolar disorder and comorbid anxiety behavior. *Psychiatry Res.* **2018**, *268*, 508–513. [[CrossRef](#)] [[PubMed](#)]
70. Kirshenbaum, G.S.; Clapcote, S.J.; Duffy, S.; Burgess, C.R.; Petersen, J.; Jarowek, K.J.; Yücel, Y.H.; Cortez, M.A.; Snead, O.C.; Vilsen, B.; et al. Mania-like behavior induced by genetic dysfunction of the neuron-specific Na⁺, K⁺-ATPase α 3 sodium pump. *Proc. Natl. Acad. Sci. USA* **2011**, *108*, 18144–18149. [[CrossRef](#)] [[PubMed](#)]
71. Fava, G.A.; Bech, P. The concept of euthymia. *Psychother. Psychosom.* **2016**, *85*, 1–5. [[CrossRef](#)]
72. El-Mallakh, R.S.; El-Masri, M.A.; Huff, M.O.; Li, X.-P.; Decker, S.; Levy, R.S. Intracerebroventricular administration of ouabain as a model of mania in rats. *Bipolar Disord.* **2003**, *5*, 362–365. [[CrossRef](#)] [[PubMed](#)]
73. Silva, R.; Mesquita, A.; Bessa, J.; Sousa, J.; Sotiropoulos, I.; Leão, P.; Almeida, O.; Sousa, N. Lithium blocks stress-induced changes in depressive-like behavior and hippocampal cell fate: The role of glycogen-synthase-kinase-3 β . *Neuroscience* **2008**, *152*, 656–669. [[CrossRef](#)] [[PubMed](#)]
74. Mohseni, G.; Ostadhadi, S.; Imran-Khan, M.; Javidan, A.N.; Zolfaghari, S.; Haddadi, N.-S.; Dehpour, A.-R. Agmatine enhances the antidepressant-like effect of lithium in mouse forced swimming test through NMDA pathway. *Biomed. Pharmacother.* **2017**, *88*, 931–938. [[CrossRef](#)]
75. Riegel, R.E.; Valvassori, S.S.; Moretti, M.; Ferreira, C.L.; Steckert, A.V.; de Souza, B.; Dal-Pizzol, F.; Quevedo, J. Intracerebroventricular ouabain administration induces oxidative stress in the rat brain. *Int. J. Dev. Neurosci.* **2010**, *28*, 233–237. [[CrossRef](#)]
76. Vitezić, D.; Pelčić, J.M.; Zupan, G.; Vitezić, M.; Ljubčić, D.; Simonić, A. NA⁺, K⁺-ATPase activity in the brain of the rats with kainic acid-induced seizures: Influence of lamotrigine. *Psychiatr. Danub.* **2008**, *20*, 269–276. [[PubMed](#)]
77. Omar, A.K.; Ahmed, K.A.; Helmi, N.M.; Abdullah, K.T.; Qarii, M.H.; Hasan, H.E.; Ashwag, A.; Nabil, A.M.; Abdu, A.-G.M.; Salama, M.S. The sensitivity of Na⁺, K⁺ ATPase as an indicator of blood diseases. *Afr. Health Sci.* **2017**, *17*, 262–269. [[CrossRef](#)] [[PubMed](#)]
78. Lu, B.; Zhang, Q.; Wang, H.; Wang, Y.; Nakayama, M.; Ren, D. Extracellular Calcium Controls Background Current and Neuronal Excitability via an UNC79-UNC80-NALCN Cation Channel Complex. *Neuron* **2010**, *68*, 488–499. [[CrossRef](#)] [[PubMed](#)]
79. Herman, L.; Houglund, T.; El-Mallakh, R.S. Mimicking human bipolar ion dysregulation models mania in rats. *Neurosci. Biobehav. Rev.* **2007**, *31*, 874–881. [[CrossRef](#)] [[PubMed](#)]
80. Budni, J.; Zomkowski, A.D.; Engel, D.; Santos, D.B.; dos Santos, A.A.; Moretti, M.; Valvassori, S.S.; Ornell, F.; Quevedo, J.; Farina, M.; et al. Folic acid prevents depressive-like behavior and hippocampal antioxidant imbalance induced by restraint stress in mice. *Exp. Neurol.* **2013**, *240*, 112–121. [[CrossRef](#)] [[PubMed](#)]
81. Banerjee, U.; Roy, S.; Roy, A.D. The intricate regulatory mechanisms of lithium on the NA⁺/K⁺ ATPase activity and redox balance in bipolar mood disorders. *J. Evol. Res. Med. Biochem.* **2016**, *2*, 12–20.
82. Sigitova, E.; Fišar, Z.; Hroudová, J.; Cikánková, T.; Raboch, J. Biological hypotheses and biomarkers of bipolar disorder. *Psychiatry Clin. Neurosci.* **2017**, *71*, 77–103. [[CrossRef](#)] [[PubMed](#)]
83. Shin, B.-K.; Kwon, S.W.; Park, J.H. Chemical diversity of ginseng saponins from Panax ginseng. *J. Ginseng Res.* **2015**, *39*, 287–298. [[CrossRef](#)] [[PubMed](#)]
84. Lichtstein, D.; Ilani, A.; Rosen, H.; Horesh, N.; Singh, S.V.; Buzaglo, N.; Hodes, A. Na⁺, K⁺-ATPase Signaling and Bipolar Disorder. *Int. J. Mol. Sci.* **2018**, *19*, 2314. [[CrossRef](#)]
85. Leaderbrand, K.; Chen, H.; Corcoran, K.A.; Guedea, A.L.; Jovasevic, V.; Wess, J.; Radulovic, J. Muscarinic acetylcholine receptors act in synergy to facilitate learning and memory. *Learn. Mem.* **2016**, *23*, 631–638. [[CrossRef](#)]
86. Butcher, A.J.; Bradley, S.J.; Prihandoko, R.; Brooke, S.M.; Mogg, A.; Bourgognon, J.-M.; Macedo-Hatch, T.; Edwards, J.M.; Bottrill, A.; Challiss, J.; et al. An Antibody Biosensor Establishes the Activation of the M1 Muscarinic Acetylcholine Receptor during Learning and Memory. *J. Biol. Chem.* **2016**, *291*, 8862–8875. [[CrossRef](#)] [[PubMed](#)]
87. Gnocchi, D.; Bruscalupi, G. Circadian Rhythms and Hormonal Homeostasis: Pathophysiological Implications. *Biology* **2017**, *6*, 10. [[CrossRef](#)]
88. Nissen, N.I.; Anderson, K.R.; Wang, H.; Lee, H.S.; Garrison, C.; Eichelberger, S.A.; Ackerman, K.; Im, W.; Miwa, J.M. Augmenting the antinociceptive effects of nicotinic acetylcholine receptor activity through lynx1 modulation. *PLoS ONE* **2018**, *13*, e0199643. [[CrossRef](#)]
89. Yang, X.F.; Xiao, Y.; Xu, M.-Y. Both endogenous and exogenous ACh plays antinociceptive role in the hippocampus CA1 of rats. *J. Neural Transm.* **2008**, *115*, 1–6. [[CrossRef](#)] [[PubMed](#)]
90. Estakhr, J.; Abazari, D.; Frisby, K.; McIntosh, J.M.; Nashmi, R. Differential Control of Dopaminergic Excitability and Locomotion by Cholinergic Inputs in Mouse Substantia Nigra. *Curr. Biol.* **2017**, *27*, 1900–1914. [[CrossRef](#)] [[PubMed](#)]

91. Martins-Silva, C.; De Jaeger, X.; Guzman, M.S.; Lima, R.D.F.; Santos, M.S.; Kushmerick, C.; Gomez, M.V.; Caron, M.G.; Prado, M.A.M.; Prado, V.F. Novel Strains of Mice Deficient for the Vesicular Acetylcholine Transporter: Insights on Transcriptional Regulation and Control of Locomotor Behavior. *PLoS ONE* **2011**, *6*, e17611. [[CrossRef](#)]
92. Cissé, Y.; Toossi, H.; Ishibashi, M.; Mainville, L.; Leonard, C.S.; Adamantidis, A.; Jones, B.E. Discharge and Role of Acetylcholine Pontomesencephalic Neurons in Cortical Activity and Sleep-Wake States Examined by Optogenetics and Juxtacellular Recording in Mice. *Eneuro* **2018**, *5*. [[CrossRef](#)]
93. Grossberg, S. Acetylcholine Neuromodulation in Normal and Abnormal Learning and Memory: Vigilance Control in Waking, Sleep, Autism, Amnesia and Alzheimer's Disease. *Front. Neural Circuits* **2017**, *11*, 82. [[CrossRef](#)]
94. Dewey, S.; Smith, G.; Logan, J.; Alexoff, D.; Ding, Y.; King, P.; Pappas, N.; Brodie, J.; Ashby, C. Serotonergic modulation of striatal dopamine measured with positron emission tomography (PET) and in vivo microdialysis. *J. Neurosci.* **1995**, *15*, 821–829. [[CrossRef](#)] [[PubMed](#)]
95. Borg, J.; André, B.; Lundberg, J.; Halldin, C.; Farde, L. Search for correlations between serotonin 5-HT_{1A} receptor expression and cognitive functions—A strategy in translational psychopharmacology. *Psychopharmacology* **2006**, *185*, 389–394. [[CrossRef](#)] [[PubMed](#)]
96. King, M.V.; Marsden, C.A.; Fone, K.C.F. A role for the 5-HT_{1A}, 5-HT₄ and 5-HT₆ receptors in learning and memory. *Trends Pharmacol. Sci.* **2008**, *29*, 482–492. [[CrossRef](#)] [[PubMed](#)]
97. Mendelsohn, D.; Riedel, W.J.; Sambeth, A. Effects of acute tryptophan depletion on memory, attention and executive functions: A systematic review. *Neurosci. Biobehav. Rev.* **2009**, *33*, 926–952. [[CrossRef](#)]
98. Daly, E.; Deeley, Q.; Hallahan, B.; Craig, M.; Brammer, M.; Lamar, M.; Cleare, A.; Giampietro, V.; Ecker, C.; Page, L.; et al. Effects of acute tryptophan depletion on neural processing of facial expressions of emotion in humans. *Psychopharmacology* **2010**, *210*, 499–510. [[CrossRef](#)]
99. Akimova, E.; Lanzenberger, R.; Kasper, S. The Serotonin-1A Receptor in Anxiety Disorders. *Biol. Psychiatry* **2009**, *66*, 627–635. [[CrossRef](#)]
100. Lucas, G.; Rymar, V.V.; Du, J.; Mnie-Filali, O.; Bisgaard, C.; Manta, S.; Lambas-Senas, L.; Wiborg, O.; Haddjeri, N.; Piñeyro, G.; et al. Serotonin₄ (5-HT₄) receptor agonists are putative antidepressants with a rapid onset of action. *Neuron* **2007**, *55*, 712–725. [[CrossRef](#)] [[PubMed](#)]
101. Fox, S.H.; Chuang, R.; Brotchie, J.M. Serotonin and Parkinson's disease: On movement, mood, and madness. *Mov. Disord.* **2009**, *24*, 1255–1266. [[CrossRef](#)]
102. Silber, B.; Schmitt, J. Effects of tryptophan loading on human cognition, mood, and sleep. *Neurosci. Biobehav. Rev.* **2010**, *34*, 387–407. [[CrossRef](#)] [[PubMed](#)]
103. Groc, L.; Choquet, D. Linking glutamate receptor movements and synapse function. *Science* **2020**, *368*, eaay4631. [[CrossRef](#)] [[PubMed](#)]
104. Suzuki, M.; Nelson, A.D.; Eickstaedt, J.B.; Wallace, K.; Wright, L.S.; Svendsen, C.N. Glutamate enhances proliferation and neurogenesis in human neural progenitor cell cultures derived from the fetal cortex. *Eur. J. Neurosci.* **2006**, *24*, 645–653. [[CrossRef](#)] [[PubMed](#)]
105. Gvirtz Probolovski, H.Z.; Dahan, A. The Potential Role of Dopamine in Mediating Motor Function and Interpersonal Synchrony. *Biomedicines* **2021**, *9*, 382. [[CrossRef](#)]
106. Jankovic, J. Dopamine depleters in the treatment of hyperkinetic movement disorders. *Expert Opin. Pharmacother.* **2016**, *17*, 2461–2470. [[CrossRef](#)] [[PubMed](#)]
107. Arias-Carrión, O.; Caraza-Santiago, X.; Salgado-Licon, S.; Salama, M.; Machado, S.; Nardi, A.E.; Menendez-Gonzalez, M.; Murillo-Rodriguez, E. Orquestric regulation of neurotransmitters on reward-seeking behavior. *Int. Arch. Med.* **2014**, *7*, 29. [[CrossRef](#)] [[PubMed](#)]
108. Solvi, C.; Baciadonna, L.; Chittka, L. Unexpected rewards induce dopamine-dependent positive emotion-like state changes in bumblebees. *Science* **2016**, *353*, 1529–1531. [[CrossRef](#)] [[PubMed](#)]
109. Taylor, A.M.; Becker, S.; Schweinhardt, P.; Cahill, C. Mesolimbic dopamine signaling in acute and chronic pain: Implications for motivation, analgesia, and addiction. *Pain* **2016**, *157*, 1194. [[CrossRef](#)] [[PubMed](#)]
110. Ott, T.; Nieder, A. Dopamine and Cognitive Control in Prefrontal Cortex. *Trends Cogn. Sci.* **2019**, *23*, 213–234. [[CrossRef](#)] [[PubMed](#)]
111. Engelhard, B.; Finkelstein, J.; Cox, J.; Fleming, W.; Jang, H.J.; Ornelas, S.; Koay, S.A.; Thiberge, S.Y.; Daw, N.D.; Tank, D.W.; et al. Specialized coding of sensory, motor and cognitive variables in VTA dopamine neurons. *Nature* **2019**, *570*, 509–513. [[CrossRef](#)]
112. Li, C.; Sugam, J.A.; Lowery-Gionta, E.G.; McElligott, Z.A.; McCall, N.; Lopez, A.J.; McKlveen, J.M.; Pleil, K.E.; Kash, T.L. Mu Opioid Receptor Modulation of Dopamine Neurons in the Periaqueductal Gray/Dorsal Raphe: A Role in Regulation of Pain. *Neuropsychopharmacology* **2016**, *41*, 2122–2132. [[CrossRef](#)]
113. Ayano, G. Dopamine: Receptors, Functions, Synthesis, Pathways, Locations and Mental Disorders: Review of Literatures. *J. Ment. Disord. Treat.* **2016**, *2*, 2. [[CrossRef](#)]
114. Zheng, L.-F.; Liu, S.; Zhou, L.; Zhang, X.-L.; Yu, X.; Zhu, J.-X. Dopamine and Gastrointestinal Motility. In *Dopamine in the Gut*; Springer: Singapore, 2021; pp. 133–202.
115. Yang, Y.-L.; Ran, X.-R.; Li, Y.; Zhou, L.; Zheng, L.-F.; Han, Y.; Cai, Q.-Q.; Wang, Z.-Y.; Zhu, J.-X. Expression of Dopamine Receptors in the Lateral Hypothalamic Nucleus and Their Potential Regulation of Gastric Motility in Rats with Lesions of Bilateral Substantia Nigra. *Front. Neurosci.* **2019**, *13*, 195. [[CrossRef](#)] [[PubMed](#)]

116. Mehan, S.; Parveen, S.; Kalra, S. Adenyl cyclase activator forskolin protects against Huntington's disease-like neurodegenerative disorders. *Neural Regen. Res.* **2017**, *12*, 290. [[CrossRef](#)] [[PubMed](#)]
117. Valvassori, S.S.; Dal-Pont, G.C.; Resende, W.R.; Varela, R.B.; Lopes-Borges, J.; Cararo, J.H.; Quevedo, J. Validation of the animal model of bipolar disorder induced by Ouabain: Face, construct and predictive perspectives. *Transl. Psychiatry* **2019**, *9*, 158. [[CrossRef](#)]
118. Valvassori, S.S.; Dal-Pont, G.C.; Varela, R.B.; Resende, W.R.; Gava, F.F.; Mina, F.G.; Budni, J.; Quevedo, J. Ouabain induces memory impairment and alter the BDNF signaling pathway in an animal model of bipolar disorder: Cognitive and neurochemical alterations in BD model. *J. Affect. Disord.* **2021**, *282*, 1195–1202. [[CrossRef](#)]
119. Kumar, N.; Sharma, N.; Khera, R.; Gupta, R.; Mehan, S. Guggulsterone ameliorates ethidium bromide-induced experimental model of multiple sclerosis via restoration of behavioral, molecular, neurochemical and morphological alterations in rat brain. *Metab. Brain Dis.* **2021**, *36*, 911–925. [[CrossRef](#)]
120. Nestler, E.J.; Hyman, S.E. Animal models of neuropsychiatric disorders. *Nat. Neurosci.* **2010**, *13*, 1161–1169. [[CrossRef](#)] [[PubMed](#)]
121. Rahi, S.; Gupta, R.; Sharma, A.; Mehan, S. Smo-Shh signaling activator purmorphamine ameliorates neurobehavioral, molecular, and morphological alterations in an intracerebroventricular propionic acid-induced experimental model of autism. *Hum. Exp. Toxicol.* **2021**, *40*, 1880–1898. [[CrossRef](#)] [[PubMed](#)]
122. Gupta, R.; Mehan, S.; Sethi, P.; Prajapati, A.; Alshammari, A.; Alharbi, M.; Al-Mazroua, H.A.; Narula, A.S. Smo-Shh Agonist Purmorphamine Prevents Neurobehavioral and Neurochemical Defects in 8-OH-DPAT-Induced Experimental Model of Obsessive-Compulsive Disorder. *Brain Sci.* **2022**, *12*, 342. [[CrossRef](#)]
123. Sharma, A.; Bhalla, S.; Mehan, S. PI3K/AKT/mTOR signalling inhibitor chrysophanol ameliorates neurobehavioural and neurochemical defects in propionic acid-induced experimental model of autism in adult rats. *Metab. Brain Dis.* **2022**, *37*, 1909–1929. [[CrossRef](#)] [[PubMed](#)]
124. Yadav, R.K.; Mehan, S.; Sahu, R.; Kumar, S.; Khan, A.; Makeen, H.A.; Al Bratty, M. Protective effects of apigenin on methylmercury-induced behavioral/neurochemical abnormalities and neurotoxicity in rats. *Hum. Exp. Toxicol.* **2022**, *41*, 09603271221084276. [[CrossRef](#)] [[PubMed](#)]
125. Sahu, R.; Mehan, S.; Kumar, S.; Prajapati, A.; Alshammari, A.; Alharbi, M.; Assiri, M.A.; Narula, A.S. Effect of alpha-mangostin in the prevention of behavioural and neurochemical defects in methylmercury-induced neurotoxicity in experimental rats. *Toxicol. Rep.* **2022**, *9*, 977–998. [[CrossRef](#)]
126. Ohta, M.; Ohta, K. Detection of myelin basic protein in cerebrospinal fluid. *Expert Rev. Mol. Diagn.* **2002**, *2*, 627–633. [[CrossRef](#)]
127. Minj, E.; Upadhayay, S.; Mehan, S. Nrf2/HO-1 Signaling Activator Acetyl-11-keto-beta Boswellic Acid (AKBA)-Mediated Neuroprotection in Methyl Mercury-Induced Experimental Model of ALS. *Neurochem. Res.* **2021**, *46*, 2867–2884. [[CrossRef](#)]
128. Mariani, S.; Di Giorgio, M.R.; Martini, P.; Persichetti, A.; Barbaro, G.; Basciani, S.; Contini, S.; Poggiogalle, E.; Sarnicola, A.; Genco, A.; et al. Inverse Association of Circulating SIRT1 and Adiposity: A Study on Underweight, Normal Weight, and Obese Patients. *Front. Endocrinol.* **2018**, *9*, 449. [[CrossRef](#)]
129. Jamali-Raeufy, N.; Mojarrab, Z.; Baluchnejadmojarad, T.; Roghani, M.; Fahanik-Babaei, J.; Goudarzi, M. The effects simultaneous inhibition of dipeptidyl peptidase-4 and P2X7 purinoceptors in an in vivo Parkinson's disease model. *Metab. Brain Dis.* **2020**, *35*, 539–548. [[CrossRef](#)] [[PubMed](#)]
130. Tiwari, A.; Khera, R.; Rahi, S.; Mehan, S.; Makeen, H.; Khormi, Y.; Rehman, M.; Khan, A. Neuroprotective Effect of α -Mangostin in Ameliorating Propionic Acid-Induced Experimental Model of Autism in Wistar Rats. *Brain Sci.* **2021**, *11*, 288. [[CrossRef](#)] [[PubMed](#)]
131. Salminen, A.; Kaarniranta, K.; Kauppinen, A. Crosstalk between Oxidative Stress and SIRT1: Impact on the Aging Process. *Int. J. Mol. Sci.* **2013**, *14*, 3834–3859. [[CrossRef](#)] [[PubMed](#)]
132. Rana, S.; Singh, L.; Mehan, S. Forskolin, ameliorates mitochondrial dysfunction in Streptozotocin induced diabetic nephropathy in rats. *Asian J. Pharm. Pharmacol.* **2018**, *5*, 199–206. [[CrossRef](#)]
133. Mehan, S.; Rahi, S.; Tiwari, A.; Kapoor, T.; Rajdev, K.; Sharma, R.; Khera, H.; Kosey, S.; Kukkar, U.; Dudi, R. Adenylate cyclase activator forskolin alleviates intracerebroventricular propionic acid-induced mitochondrial dysfunction of autistic rats. *Neural Regen. Res.* **2020**, *15*, 1140. [[CrossRef](#)] [[PubMed](#)]
134. Mehan, S.; Kapoor, T. Neuroprotective Methodologies in the Treatment of Multiple Sclerosis Current Status of Clinical and Pre-clinical Findings. *Curr. Drug Discov. Technol.* **2021**, *18*, 31–46. [[CrossRef](#)]
135. Dudi, R.; Mehan, S. Neuroprotection of brain permeable Forskolin ameliorates behavioral, biochemical and histopathological alterations in rat model of intracerebral hemorrhage. *Pharmaspire* **2018**, *10*, 68–86.
136. Deshmukh, R.; Sharma, V.; Mehan, S.; Sharma, N.; Bedi, K. Amelioration of intracerebroventricular streptozotocin induced cognitive dysfunction and oxidative stress by vinpocetine—A PDE1 inhibitor. *Eur. J. Pharmacol.* **2009**, *620*, 49–56. [[CrossRef](#)] [[PubMed](#)]
137. Mehan, S.; Meena, H.; Sharma, D.; Sankhla, R. JNK: A Stress-Activated Protein Kinase Therapeutic Strategies and Involvement in Alzheimer's and Various Neurodegenerative Abnormalities. *J. Mol. Neurosci.* **2011**, *43*, 376–390. [[CrossRef](#)]

138. Mehan, S.; Khera, H.; Awasthi, A. Myocardial preconditioning potential of hedgehog activator purmorphamine (smoothened receptor agonist) against ischemia-reperfusion in deoxycortisone acetate salt-induced hypertensive rat hearts. *J. Pharmacol. Pharmacother.* **2019**, *10*, 47. [[CrossRef](#)]
139. Rezin, G.T.; Scaini, G.; Gonçalves, C.L.; Ferreira, G.K.; Cardoso, M.R.; Ferreira, A.G.; Streck, E.L. Evaluation of Na⁺, K⁺-ATPase activity in the brain of young rats after acute administration of fenproporex. *Braz. J. Psychiatry* **2013**, *36*, 138–142. [[CrossRef](#)] [[PubMed](#)]